University of South Africa ETD Grobler, J. (2010)

HYPERNUCLEAR BOUND STATES WITH TWO Λ-PARTICLES

by

JONATHAN GROBLER

submitted in accordance with the requirements for the degree of

MASTER OF SCIENCE

in the subject

PHYSICS

at the

UNIVERSITY OF SOUTH AFRICA

SUPERVISOR: PROF S A RAKITYANSKY

NOVEMBER 2009

University of South Africa ETD Grobler, J. (2010)

Declaration

I, the undersigned, declare that *Hypernuclear Bound States with two* Λ*-particles* is my own work and that all the sources that I have used or quoted have been indicated and acknowledged by means of complete references. This work has not been previously submitted, either in its entirety, or in part, for a degree at this, or at any another tertiary institution.

Signature:_____ Date:_____

University of South Africa ETD Grobler, J. (2010)

Summary

The double Λ hypernuclear systems are studied within the context of the hyperspherical approach. Possible bound states of these systems are sought as zeros of the corresponding three-body Jost function in the complex energy plane. Hypercentral potentials for the system are constructed from known potentials in order to determine bound states of the system. Calculated binding energies for double-Λ hypernuclei having $A = 4 - 20$, are presented.

Keywords: Jost function, bound state, Λ-particle, Λ-Λ interaction, hypernucleus, hyperspherical harmonics, complex rotation, hypercentral potential

University of South Africa ETD Grobler, J. (2010)

Acknowledgements

My heartfelt gratitude and appreciation goes to the following persons for their guidance and support:

My wife Ruth, Michael, Rachel and Prof. S. A. Rakityansky.

In loving memory of my mother.

University of South Africa ETD Grobler, J. (2010)

List of Figures

University of South Africa ETD Grobler, J. (2010)

University of South Africa ETD Grobler, J. (2010)

List of Tables

University of South Africa ETD Grobler, J. (2010)

Contents

University of South Africa ETD Grobler, J. (2010)

University of South Africa ETD Grobler, J. (2010)

Chapter 1

Introduction

Until 1947, it was thought that the only building blocks of nuclei were protons and neutrons, bound together by nuclear forces. It was in this year that the pioneering work of C.F. Powell [1], who developed the nuclear emulsion technique, produced evidence for the existence of mesons. The evidence produced by Powell included what is now known as the π meson. These discoveries initiated elementary particle physics as a separate branch of physics and established the nuclear emulsion technique as a recognised method in the search for elementary particles.

In 1952, using the nuclear emulsion technique, Marian Dansyz and Jerzy Pniewski [2] came across a surprising case of two stars connected by a thick track. Their analysis led them to conclude that the experimental evidence depicted a hypernucleus, in their particular case, a nucleus consisting of a Λ-hyperon and nucleons. Up to, and until 1955, many other cases of hypernuclei were announced [3]. These new dicoveries posed new fundamental questions concerning the existence, creation and disintegration of the Λ-hyperon, questions which would pave the way for exciting new developments in the area of elementary particles and their interactions.

University of South Africa ETD Grobler, J. (2010)

The first double hypernucleus was discovered in Warsaw, in 1962 [4], using a nuclear emulsion irradadiated by a beam of kaons (K^--mesons), and the second at Brookhaven National Laboratory in 1966 [5]. Further searches for double hypernuclei, including the use of spectrometers, were unsuccessful with none being discovered for over thirty years. Finally, in 1991, in an experiment performed with K^--beams at the KEK Proton Synchorotron in Tokyo [6], the next double hypernucleus was discovered.

Hypernuclei are of great importance as they provide the only means of obtaining information on the Λ-Λ interaction, notably the binding energy of two Λ-hyperons, $B_{\Lambda\Lambda}$, and the Λ-Λ interaction energy, $\Delta B_{\Lambda\Lambda}$. The interaction energy can be obtained from the mass of double hypernuclei using the formula [7]

$$\Delta B_{\Lambda\Lambda}({}^{A}_{\Lambda\Lambda}\mathrm{Z}) = B_{\Lambda\Lambda}({}^{A}_{\Lambda\Lambda}\mathrm{Z}) - 2B_{\Lambda}({}^{A-1}_{\Lambda\Lambda}\mathrm{Z}), \tag{1.1}$$

where the superscript A indicates the total number of baryons. For example, ${}^{6}_{\Lambda\Lambda}$He is a bound system ($ppnn\Lambda\Lambda$).

The Λ-Λ interaction may also provide valuable insight into the details of neutron stars [8], where hyperons are seen to play an important role in the core region of these stars. The structure of the hypernucleus also provides valuable information on the hyperon-nucleon interaction. Little is currently known about hyperon-nucleon interactions with more theoretical and experimental work being required for an accurate description of them. There are numerous reasons which motivate hypernuclear physics research: A detailed, consistent understanding of the quark aspect for bayron-bayron interactions is needed; extension of the three-dimensional hypernuclear chart; impurity effects in nuclear structure; nuclear medium effects of bayrons; the study of

University of South Africa ETD Grobler, J. (2010)

strangeness in astro physics; and the production of exotic hypernuclei beyond the normal neutron/proton drip lines.

The binding energies of double hypernuclei have been studied as far back as 1960, with the aim of gaining more information on the Λ-Λ interaction [9]. These studies were theoretical in nature and unsuccessful in accurately determining the binding energies of two hyperons. Recent experimental work performed at the KEK proton synchrotron [7], using the 1.66 GeV/c separated K^- meson beam, unveiled important information about the ${}^{6}_{\Lambda\Lambda}$He double hypernucleus. An event of seminal importance, a mesonically decaying double hypernucleus, was identified and termed the "Nagara" event [7]. The results of the experimental work provided the first-ever, reliable information on the binding energy of ${}^{6}_{\Lambda\Lambda}$He.

After the *Nagara* event, there were numerous other attempts to establish whether ${}^{4}_{\Lambda\Lambda}$He is a stable bound state against strong decay [10, 11]. The inclusion of a set of baryon-baryon interactions, consistent with experimental data, was used [10] to predict a stable state of ${}^{4}_{\Lambda\Lambda}$H. The results of this work showed that with the inclusion of a set of baryon-baryon intractions among the octet baryons in the $S = 0, -1$ and -2 strangeness sectors (which is consistent with the *Nagara* event as well as the experimental binding energies of $S = 0$ and -1 s-shell hypernuclei) one can predict a stable bound state of ${}^{4}_{\Lambda\Lambda}$He. Bound state solutions for ${}^{4}_{\Lambda\Lambda}$H, ${}^{5}_{\Lambda\Lambda}$H, ${}^{5}_{\Lambda\Lambda}$He were also determined as well as Λ-Λ separation energies of $A = 4$, $S = -2$ hypernuclei [10].

In addition to the *Nagara* event, the "Demachi-Yanagi" event [12] revealed more information about hypernuclei. The binding energy of ${}^{10}_{\Lambda\Lambda}$Be was evaluated as $B_{\Lambda\Lambda} = 12.33^{+0.35}_{-0.21}$ MeV. However, it was not certain at the time whether the state observed was a ground state or an excited state. Later,

University of South Africa ETD Grobler, J. (2010)

systematic four-body calculations for ${}^{6}_{\Lambda\Lambda}$He were performed [13] which showed that the *Demachi-Yanagi* event may be interptreted as the 2^+ state of ${}^{10}_{\Lambda\Lambda}$Be.

The microscopic cluster model is found to be most useful in understanding the structure of light hypernuclei and is established as an important feature of hypernuclear systems and has been successful in describing the shell structure of hypernuclei [14, 15, 16]. In the cluster model, antisymmetrization of nucleons is properly taken into account with wave functions treating constituent clusters as composites. The cluster model has also been successful in describing the nuclear response to the addition of the Λ-hyperon which is uninhibited by the Pauli blocking effect [12].

The Gaussian expansion method [17] has enjoyed recent success in the area of three- and four-body structure calculations. The method employs a set of Gaussian basis functions which form a set in coordinate space. These basis functions enable description of both the short-range and the long-range asymptotic behaviour of the wave function for bound systems and scattering states [12].

Despite the success of the Gaussian expansion method and the Cluster model, the results of these methods are acknowledged as predictions, especially the energy spectra of double Λ with $A = 6 - 10$. The *Nagara* and *Demachi-Yanagi* events remain the most accurate and reliable sources of experimental evidence for the binding energies of double Λ-hypernuclei. As these results serve as the only reliable source of data, they impose natural constraints on binding energy calculations of ${}^{6}_{\Lambda\Lambda}$He and ${}^{10}_{\Lambda\Lambda}$Be. Due to the lack of confirmed experimental evidence, forthcoming experiments are expected to reveal further aspects of hypernuclear systems [18].

What about scattering experiments using Λ-particles, one may ask. Un-

University of South Africa ETD Grobler, J. (2010)

fortunately, due to the short lifetime of the Λ-particle, its scarcity and low intensity beams that can be obtained from them, it is difficult to conduct scattering experiments using Λ-particles. Targets which consist of Λ-particles are not readily available, which makes scattering experiments difficult. Hyperon-nucleon interactions and hyperon-hyperon scattering in free space is also very difficult.

In recent work [19], three-body resonances of the Λnn and ΛΛn hypernuclear systems were sought as zeros of the corresponding Jost functions. The hyperspherical approach with local two-body S-wave potentials describing nn, Λn, and Λ-Λ interactions was used. It was found that the positions of the resonances were sensitive to the choice of the Λn-potential. It was also found that bound states appear when the potential strength was increased by approximately 50%, implying that the Jost function zeros crossed the threshold and moved into the real negative axis. The method was successful in locating resonances, but did not include a search for bound states of hypernuclei containing two Λ-hyperons, which is the subject of this work.

We aim to develop a theoretical model of a ΛΛ hypernuclear system, with a view to determining how strong the the Λ-Λ interaction is based on comparison with the experimental results obtained in the *Nagara* and the *Demachi-Yangi* events. We also aim to determine binding energies for $A = 4 - 20$ hypernuclei. Our calculations reproduce the binding energy of ${}^{6}_{\Lambda\Lambda}\mathrm{He}$ and therefore we hope that the results which we obtained for the other ΛΛ hypernuclei are also realistic. They can be considered as estimates for future experiments.

We consider the ΛΛ-nucleus system in the three-body model: nuclear core plus two Λ-particles. The three-body wave function is expanded in terms of

University of South Africa ETD Grobler, J. (2010)

hyperspherical harmonics. The resulting system of hyperradial equations is truncated to a single Schrödinger-like equation.

We reduce the second-order Schrödinger Equation of the system to a single pair of first-order differential equations. Each of these first-order differential equations is then solved numerically as a boundary-value problem to determine the Jost function. The Jost function is then used to locate the bound states for the hypernuclear system.

This work is structured as follows: In Chapter 2 we describe the Λ-particle and the hypernucleus. In Chapter 3 we develop a model which consists of two Λ-particles in the nucleus. Here we derive the Hamiltonian and the Schrödinger Equation for the system. In Chapter 4 we describe the Jost function method for solving the Schrödinger Equation derived in Chapter 3, methods for locating bound states for $\Lambda\Lambda$ hypernuclear systems, the Minimal Approximation and Complex Rotation. In Chapter 5 we present and discuss the results of our method, and in Chapter 6 we state the conclusion.

University of South Africa ETD Grobler, J. (2010)

Chapter 2

Hypernuclear Physics

The *Nagara* event involved the production of Ξ^--hyperons, measurements of the position and angles of entry of Ξ^--hyperons, and analysis of the experimental results using measured lengths and angles of the tracks. The kinematics of all possible decay modes was also investigated. The event was interpreted as the sequential weak decay of ${}^{6}_{\Lambda\Lambda}$He, the lightest triply-closed s-shell nuclear system [7]. The most probable weighted mean value for the binding energy was determined, $B_{\Lambda\Lambda} = 7.25 \pm 0.19^{+0.18}_{-0.11}$ MeV, and the interaction energy, $\Delta B_{\Lambda\Lambda} = 1.10 \pm 0.20^{+0.18}_{-0.11}$ MeV, was also determined. Binding energies for two Λ-hyperons, $B_{\Lambda\Lambda}$, and the Λ-Λ interaction energy, $\Delta B_{\Lambda\Lambda}$, were also presented [7]. These are given in Table 2.1.

Four-body cluster model calculations have been extensively used to study the structure of $\Lambda\Lambda$ hypernuclear systems. In these structure calculations [12], the $\Lambda\Lambda$ hypernuclear systems ${}^{7}_{\Lambda\Lambda}$He, ${}^{7}_{\Lambda\Lambda}$Li, ${}^{8}_{\Lambda\Lambda}$Li, ${}^{9}_{\Lambda\Lambda}$Li, ${}^{9}_{\Lambda\Lambda}$Be, and ${}^{10}_{\Lambda\Lambda}$Be were studied within the framework of an $(\alpha + x + \Lambda + \Lambda)$ four-body model with $x = 0, n, p, d, t, {}^{4}_{\Lambda}$He and α, respectively. Here, the d, $t({}^{3}$He) and α clusters were assumed to be inert, having the $(0s)^2$, $(0s)^3$, and $(0s)^4$ shell-model configurations, respectively, with spins $s(= 1, 1/2, \text{ or } 0)$, respectively.

University of South Africa ETD Grobler, J. (2010)

Cluster models have also been extended to more general cases where the nuclear core is well represented. Recent calculations for the $A = 7 - 9$ Λ species have been presented for the first time [12] and a summary of the calculated ground state energies for $\Lambda\Lambda$ hypernuclear species is given in Table 2.2.

Hypernucleus	$B_{\Lambda\Lambda}$ [MeV]	$\Delta B_{\Lambda\Lambda}$ [MeV]
${}^{5}_{\Lambda\Lambda}$He	7.1 ± 0.5	2.4 ± 0.5
${}^{6}_{\Lambda\Lambda}$He	6.9 ± 0.6	0.6 ± 0.6
${}^{7}_{\Lambda\Lambda}$He	6.3 ± 0.7	-2.0 ± 0.7
${}^{8}_{\Lambda\Lambda}$He	7.7 ± 0.8	-6.3 ± 0.8
${}^{9}_{\Lambda\Lambda}$He	13.4 ± 0.5	-0.9 ± 0.5
${}^{9}_{\Lambda\Lambda}$He	6.4 ± 0.8	-7.9 ± 0.8

Table 2.1: Binding energies for two Λ-hyperons, $B_{\Lambda\Lambda}$, and Λ-Λ interaction energy, $\Delta B_{\Lambda\Lambda}$. The errors on $B_{\Lambda\Lambda}$ do not include those of the binding energies of single hypernuclei. Values are taken from Ref. [7].

Hypernucleus	$B_{\Lambda\Lambda}$ [MeV]
${}^{7}_{\Lambda\Lambda}$Li	9.45
${}^{8}_{\Lambda\Lambda}$Li	11.44
${}^{9}_{\Lambda\Lambda}$Li	14.55
${}^{10}_{\Lambda\Lambda}$Be	15.14

Table 2.2: Calculated energies of the ground states of $A = 7 - 10$ based on the $(\alpha + x + \Lambda + \Lambda)$ four-body model ($x = 0, n, p, d, t,$ ${}^{4}_{\Lambda}$He and α). Values are taken from Ref. [12]

University of South Africa ETD Grobler, J. (2010)

2.1 The Λ-particle

The first Λ-particle was discovered in 1947 during research of cosmic ray interactions [20]. This led to a number of further discoveries, notably the principle of the conservation of strangeness and the strange quark.

The Λ-particle contains an up quark, a down quark, and a strange quark. The Λ-particle is the lightest of the hyperons with a rest mass of 1115.684 MeV/c^2 and a mean lifetime of 2.60×10^{-10}s, which is consistent with weak decay [21]. The Λ-particle also has the properties listed in Table 2.3.

Λ-particle property	Quantum Number
Isospin (I)	0
Spin (Parity)	$1/2^+$
Charge (Q)	0
Strangeness (S)	-1
Charm (C)	0
Bottomness (B)	0

Table 2.3: Properties of the Λ-particle. Values are taken from Ref. [21].

The Λ-particle decays into a nucleon through a weak interaction process. The strangeness quantum number, S, changes by one unit during the decay process, hence S is not conserved during the process. The decay modes of the Λ-hyperon are given in Table 2.4

As the Λ-particle is shortlived, the study of Λ-particles bound in the nucleus may provide valuable information about the interaction between hyperons (Y) and nucleons (N).

As we know, neither beams nor targets of Λ-particles are readily available,

University of South Africa ETD Grobler, J. (2010)

Λ decay mode	Fraction [%]
$p + \pi^-$	(63.9 ± 0.5)
$n + \pi^0$	(35.8 ± 0.5)
$n + \gamma$	$(1.75 \pm 0.15) \times 10^{-3}$
$p + \pi^- + \gamma$	$(8.4 \pm 1.4) \times 10^{-4}$
$p + e^- + \bar{\nu}_e$	$(8.32 \pm 0.14) \times 10^{-4}$
$p + \mu^- + \bar{\nu}_\mu$	$(1.57 \pm 0.35) \times 10^{-4}$

Table 2.4: Λ decay modes. Values are taken from Ref. [22]

which makes scattering experiments with Λ-particles difficult. However, in practice Λ-particles may be produced by passing a beam of kaons into a liquid hydrogen target [21]. In this process, Λ-particles are produced in the reaction

$$K^- + p \rightarrow {}^{A}_{\Lambda}X + \pi^+,$$

where p denotes the proton and π^+ the π-meson with positive electric charge. As with nn scattering, Λp scattering may be characterized by two parameters, the scattering length a and the effective range r_0. The scattering data obtained favor the values $a = -1.8 \pm 0.2$ fm and $r_0 = 3.16 \pm 0.52$ fm [21].

Another way of examining nuclear interactions of Λ-particles is through hypernuclei where a neutron is replaced with a Λ-particle. This is achieved in scattering experiments using a beam of K^- and with nuclei as targets [21]. This kind of reaction is indicated by

$$K^- + n \rightarrow {}^{A}_{\Lambda}X + \pi^-,$$

where Λ-particles produced at low momentum have a high probability of remaining bound to the nucleus. As the Λ-particles are not limited by the

University of South Africa ETD Grobler, J. (2010)

Pauli principle, they can drop quickly to the 1s shell state, despite the fact that there may already be two neutrons in that state. The Λ-particle may stay in the 1s state until it decays, according to

$$\Lambda \rightarrow p + \pi^{-},$$

or

$$\Lambda \rightarrow n + \pi^{0}.$$

The Λ-particle may alternatively undergo a strangeness-changing weak reaction with either the proton or the neutron

$$\Lambda + n \rightarrow n + n$$

$$\Lambda + p \rightarrow n + p.$$

2.2 The Hypernucleus

A hypernucleus is a nucleus which contains at least one hyperon in addition to protons and neutrons. In this work we consider Λ-hypernuclei.

The addition of the Λ-hyperon to the nucleus has the effect of stabilising the nucleus, due to its "glue-like"role, with the nuclear core undergoing sizable dynamic changes [12]. The addition of the the Λ-hyperon to the nucleus also has the effect of shrinking the nucleus, and may make a normal unbound nucleus bound. For example, ^{10}Li is known to be unbound, but $^{10}_{\Lambda}$Li is bound [23], with a Λ-separation energy of ≈ 12.8 MeV.

One of the main differences between ordinary nuclear physics and hypernuclear physics is seen in the structure of $^{4}_{\Lambda}$He, which has a nucleus consisting

University of South Africa ETD Grobler, J. (2010)

of two protons, one neutron and one Λ-particle. In the ground state of ^{4}H, all particles are required to have their spins oriented in opposite directions in order to satisfy the Pauli principle. However, for $^{4}_{\Lambda}$He, no such rule applies as the spins of the particles can be either antiparallel or parallel [21]. This difference may prove to be a distinctive feature of binging energy curves for hypernuclei.

Generalized mass formulae for normal ($S = 0$) and strange ($S \neq 0$) nuclei have also been developed [23] in the experimental search for Λ-Λ separation energies. For example, the binding energy, B, is given by

$$B(A,Z) = a_v A - a_s A^{-2/3} - a_c Z(Z-1)A^{-1/3} - a_{sym}(N-Z_c)^2 A^{-1}\Big[1 + \exp(-A/17)\Big] + \delta_{new} - 48.7|S|A^{-2/3} - n_y[0.0035 m_y - 26.7]$$

where, n_y represents the number of hyperons in the nucleus, m_y is the hyperon mass in MeV, A is the total number of baryons ($A = N + Z_c + n_y$), Z_c is the number of protons ($Z = Z_c + n_y q$) and q represents the hyperon charge number with proper sign ($q = -1, 0, 1$). The terms $a_v A$, $-a_s A^{-2/3}$, and $-a_c Z(Z-1)A^{-1/3}$ are of the same form as that used in the binding energy for normal nuclei [21]. The pairing energy term δ has the form $\delta_{new} = \delta[1 - \exp(-A/30)]$.

If Λ-particles were stable like nucleons, then Λ-hypernuclei would not decay and would be more stable than ordinary nuclei. As Λ-particles are not stable, the hypernucleus decays in a time of about 2.60×10^{-10}s. The decay process can be observed by using emulsions exposed to cosmic radiation or in experiments with accelerators using secondary kaon beams or secondary pion beams. In the case of secondary pion beams, it is possible to measure the Λ-particle binding energy in the hypernucleus that has been created. In the

University of South Africa ETD Grobler, J. (2010)

case of ${}^{4}_{\Lambda}$He, the binding energy of the Λ-particle in the ground state is 2.39 MeV. The binding energy is found to increase linearly with A for the light nuclei ($A \leq 16$) due to the Λ-particle interacting with all of the nucleons, not limited by the Pauli principle [21].

Hypernuclei can be produced in various ways, one of which is the capture of a negative kaon, K^-, by the nucleus. The reaction is expressed as

$$K^- + {}^{A}X \rightarrow {}^{A}_{\Lambda}X + \pi^-,$$

where the target of ${}^{4}_{A}$He may produce ${}^{A}_{\Lambda}$He, a nucleus consisting of four bayrons (two protons, one neutron, and one Λ. Here, A indicates the number of bayrons and π^- the π-meson which has a negative electric charge.

University of South Africa ETD Grobler, J. (2010)

Chapter 3

Model

3.1 Two Λ-particles in the Nucleus

The Λ-hypernucleus we consider consists of two Λ-particles and A nucleons. We reduce this $(A+2)$ problem to a three-body problem by considering the nucleus as a structureless core.

The hypernuclear system under consideration consists of two Λ-particles of mass m_Λ, each with spin 1/2, and the nucleus of mass M. We consider two Λ-particles with a view to exploring the Λ-Λ interaction. Also, we choose known Λ-nucleus single-particle potentials [24] to describe the interaction between the two Λ-particles and the nucleus as well as the Λ-Λ interaction.

The spatial configuration of two Λ-particles inside a nucleus is depicted in Figure 3.1, where we have employed the hyperspherical coordinate system. The nucleus is taken to be much heavier than each of the Λ-particles. If we take, for example, ^{7}Li which has an atomic mass of 7.016003 MeV/c^2 [21], we see that it exceeds that of the Λ-particle by a factor of about 6. Hence, we take $M \gg m_\Lambda$, and we ignore the motion of the nucleus.

University of South Africa ETD Grobler, J. (2010)

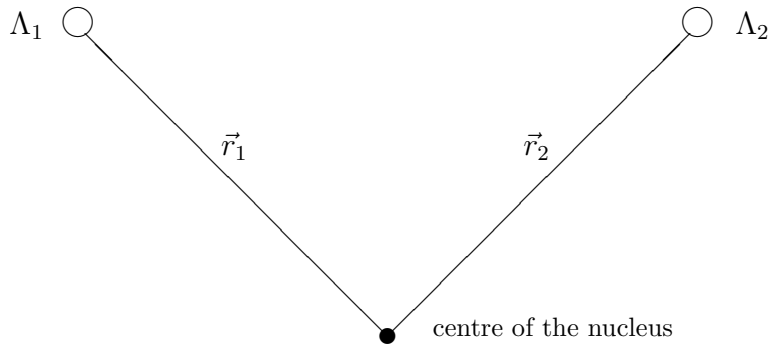

Figure 3.1: Spatial configuration of two Λ-particles in the nucleus.

3.2 The Hyperspherical Coordinate System

Various sets of coordinate systems can be used to represent a system containing more than one particle. For example, the Cartesian coordinate system can be used to represent a system of two vectors. Such a system will contain six variables with each variable ranging from $-\infty$ to $+\infty$. This is not convenient for our purposes as all of the variables are infinite and there are six variables.

The hyperspherical coordinate system, however, provides a convenient way of representing a system of several particles. A wave function dependent on one vector can be expanded in terms of spherical harmonics. Similarily, a wave function dependent on two vectors, the simplest type of hyperspherical system, can be expanded in terms of hyperspherical harmonics. The primary advantage of the hyperspherical approach is that it can be easily extended to a system containing more than two particles, such as our system.

In Figure 3.2 the variables r_1 and r_2 vary over the infinite intervals

$$0 \leq r_1 \leq \infty, \tag{3.1}$$

University of South Africa ETD Grobler, J. (2010)

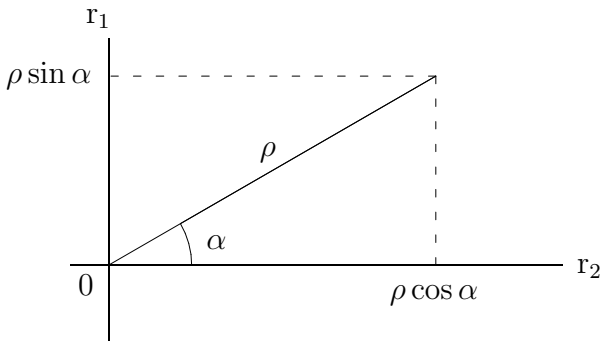

Figure 3.2: r_1 and r_2 in the polar plane. r_1 and r_2 vary over infinite intervals.

and

$$0 \leq r_2 \leq \infty. \tag{3.2}$$

All points in the first quadrant of the polar plane can be specified either in terms of polar coordinates (ρ, α) or in pairs (r_1, r_2). The two forms are related as follows

$$\rho = \sqrt{r_1^2 + r_2^2} \Leftrightarrow r_1 = \rho \cos\alpha \qquad \tan\alpha = \left(\frac{r_2}{r_1}\right) \Leftrightarrow r_2 = \rho \sin\alpha. \tag{3.3}$$

It can be seen from (3.3) that the hyperradius becomes small when the distance between the particles is small and large when the distance between the particles is large. Hence, the hyperradius, ρ, represents the collective size of the system.

3.3 Hamiltonian of the System

The Hamiltonian for a single Λ-particle of mass m_Λ, moving in the force field of the nucleus, $V(r)$, has the form

$$H = -\frac{\hbar^2}{2m_\Lambda}\vec{\nabla}_r^2 + V(r). \tag{3.4}$$

University of South Africa ETD Grobler, J. (2010)

The potential, $V(r)$, is rotationally invariant, depending only on the distance r from the centre of force, which is chosen to be the centre of the nucleus. Hence, the potential $V(r)$ is a central potential. As we have assumed a central potential, the wave function can be factored into both radial and angular parts.

The Hamiltonian (3.4) is easily extended for the case of two Λ-particles,

$$H = -\frac{\hbar^2}{2m_\Lambda}\left(\vec{\nabla}^2_{\vec{r}_1} + \vec{\nabla}^2_{\vec{r}_2}\right) + \Big[V_{\Lambda\Lambda}(\mid \vec{r}_1 - \vec{r}_2 \mid) + V_1(r_1) + V_2(r_2)\Big], \tag{3.5}$$

where

$$V_{\Lambda\Lambda}(\mid \vec{r}_1 - \vec{r}_2 \mid) \tag{3.6}$$

is the interaction potential between the two Λ-particles; $-\hbar^2\vec{\nabla}^2_{\vec{r}_1}/2m_\Lambda$ and $-\hbar^2\vec{\nabla}^2_{\vec{r}_2}/2m_\Lambda$ are the kinetic energy operators for Λ-particles 1 and 2, respectively; and $V_1(r_1)$ and $V_2(r_2)$ are the interaction potentials for each of the two Λ-particles with the nucleus.

For the sake of convenience, we recast the Hamiltonian (3.5) in terms of hypersperical coordinates, considering each term on the right-hand side of (3.5) individually. We begin with the operator $\vec{\nabla}^2_{\vec{r}}$ in (3.5).

The operator $\vec{\nabla}^2_{\vec{r}}$, can be written in spherical coordinates as

$$\vec{\nabla}^2_r = \frac{1}{r^2}\frac{\partial}{\partial r}\left(r^2\frac{\partial}{\partial r}\right) - \frac{\vec{\ell}^2}{r^2}. \tag{3.7}$$

Subsituting (3.7) into the term $\left(\vec{\nabla}^2_{\vec{r}_1} + \vec{\nabla}^2_{\vec{r}_2}\right)$, we obtain

$$\left(\vec{\nabla}^2_{\vec{r}_1} + \vec{\nabla}^2_{\vec{r}_2}\right) = \frac{1}{r_1^2}\frac{\partial}{\partial r_1}\left(r_1^2\frac{\partial}{\partial r_1}\right) + \frac{1}{r_2^2}\frac{\partial}{\partial r_2}\left(r_2^2\frac{\partial}{\partial r_2}\right) - \frac{\vec{\ell}^2_{\vec{r}_1}}{r_1^2} - \frac{\vec{\ell}^2_{\vec{r}_2}}{r_2^2}, \tag{3.8}$$

where the angular momentum operators $\vec{\ell}^2_{\vec{r}_1}$ and $\vec{\ell}^2_{\vec{r}_2}$ satisfy the normalized eigenfunction equations of spherical harmonics

$$\vec{\ell}^2_{\vec{r}_1} = Y_{\ell_1 m_1} = \ell_1(\ell_1+1)Y_{\ell_1 m_1}, \tag{3.9}$$

University of South Africa ETD Grobler, J. (2010)

and

$$\vec{\ell}^{\,2}_{\vec{r}_2} = Y_{\ell_2 m_2} = \ell_2(\ell_2+1)Y_{\ell_2 m_2}. \tag{3.10}$$

The total angular momentum of the system is conserved and is a constant of the motion. Noting also that

$$\frac{1}{r^2}\frac{\partial}{\partial r}\Big(r^2\frac{\partial}{\partial r}\Big) = \frac{\partial^2}{\partial r^2} + \frac{2}{r}\frac{\partial}{\partial r}, \tag{3.11}$$

and substituting (3.11) into (3.8), we obtain

$$\Big(\vec{\nabla}^2_{\vec{r}_1} + \vec{\nabla}^2_{\vec{r}_2}\Big) = \Big(\frac{\partial^2}{\partial r_1^2} + \frac{\partial^2}{\partial r_2^2}\Big) + 2\Big(\frac{1}{r_1}\frac{\partial}{\partial r_1} + \frac{1}{r_2}\frac{\partial}{\partial r_2}\Big) - \frac{\vec{\ell}^{\,2}_{\vec{r}_1}}{r_1^2} - \frac{\vec{\ell}^{\,2}_{\vec{r}_2}}{r_2^2}. \tag{3.12}$$

The first term on the right hand side of (3.12) is a two-dimensional Laplacian which can be written in terms of polar coordinates as

$$\Big(\frac{\partial^2}{\partial r_1^2} + \frac{\partial^2}{\partial r_2^2}\Big) = \frac{1}{\rho}\frac{\partial}{\partial \rho}\Big(\rho\frac{\partial}{\partial \rho}\Big) + \frac{1}{\rho^2}\frac{\partial^2}{\partial \alpha^2}, \tag{3.13}$$

and the second term on the right hand side of (3.12) can also be written in terms of polar coordinates as

$$\Big(\frac{1}{r_1}\frac{\partial}{\partial r_1} + \frac{1}{r_2}\frac{\partial}{\partial r_2}\Big) = \Big(\frac{\partial\rho}{\partial r_1}\frac{\partial}{\partial \rho}\Big) + \Big(\frac{\partial\alpha}{\partial r_1}\frac{\partial}{\partial \alpha}\Big) + \Big(\frac{\partial\rho}{\partial r_2}\frac{\partial}{\partial \rho}\Big) + \Big(\frac{\partial\alpha}{\partial r_2}\frac{\partial}{\partial \alpha}\Big). \tag{3.14}$$

The individual terms on the right hand side of (3.14) can be written as,

$$\frac{\partial\rho}{\partial r_1} = \frac{\partial}{\partial r_1}\Big(\sqrt{r_1^2+r_2^2}\Big) = \frac{1}{2}\Big(r_1^2+r_2^2\Big)^{\frac{1}{2}-1}\frac{\partial}{\partial r_1}(r_1^2) = \cos\alpha, \tag{3.15}$$

$$\frac{\partial\alpha}{\partial r_1} = \frac{\partial}{\partial r_1}\left[\arctan\left(\frac{r_2}{r_1}\right)\right] = -\frac{r_2}{r_1^2+r_2^2} = -\frac{1}{\rho}\sin\alpha, \tag{3.16}$$

$$\frac{\partial\rho}{\partial r_2} = \frac{\partial}{\partial r_2}\Big(\sqrt{r_1^2+r_2^2}\Big) = \frac{1}{2}\Big(r_1^2+r_2^2\Big)^{\frac{1}{2}-1}\frac{\partial}{\partial r_1}(r_2^2) = \sin\alpha, \tag{3.17}$$

and

$$\frac{\partial\alpha}{\partial r_2} = \frac{\partial}{\partial r_2}\left[\arctan\left(\frac{r_2}{r_1}\right)\right] = \frac{r_1}{r_1^2+r_2^2} = \frac{1}{\rho}\cos\alpha. \tag{3.18}$$

University of South Africa ETD Grobler, J. (2010)

Substituting (3.15) to (3.18) into (3.14), we obtain

$$\begin{aligned}\Big(\frac{1}{r_1}\frac{\partial}{\partial r_1}+\frac{1}{r_2}\frac{\partial}{\partial r_2}\Big) &= \frac{1}{r_1}\Big(\cos\alpha\frac{\partial}{\partial\rho}-\frac{1}{\rho}\sin\alpha\frac{\partial}{\partial\alpha}\Big)+\frac{1}{r_2}\Big(\sin\alpha\frac{\partial}{\partial\rho}+\frac{1}{\rho}\cos\alpha\frac{\partial}{\partial\alpha}\Big)\\ &= \frac{1}{\rho}\frac{\partial}{\partial\rho}-\frac{1}{\rho^2}\tan\alpha\frac{\partial}{\partial\alpha}+\frac{1}{\rho}\frac{\partial}{\partial\rho}+\frac{1}{\rho^2}\cot\alpha\frac{\partial}{\partial\alpha}\\ &= \frac{2}{\rho}\frac{\partial}{\partial\rho}+\frac{1}{\rho^2}(\cot\alpha-\tan\alpha)\frac{\partial}{\partial\alpha}.\end{aligned}$$

Since,

$$\cot\alpha-\tan\alpha=2\cot 2\alpha,$$

hence, the second term on the right hand side of (3.12) becomes

$$2\Big(\frac{1}{r_1}\frac{\partial}{\partial r_1}+\frac{1}{r_2}\frac{\partial}{\partial r_2}\Big)=\frac{4}{\rho}\frac{\partial}{\partial\rho}+\frac{4}{\rho^2}\cot 2\alpha\frac{\partial}{\partial\alpha}. \tag{3.19}$$

The first term on the right hand side of (3.13) can be written as

$$\begin{aligned}\frac{1}{\rho}\frac{\partial}{\partial\rho}\Big(\rho\frac{\partial}{\partial\rho}\Big) &= \frac{1}{\rho}\Big(\frac{\partial}{\partial\rho}\frac{\partial}{\partial\rho}\rho\Big)+\rho\Big(\frac{\partial}{\partial\rho}\frac{\partial}{\partial\rho}\Big)\\ &= \frac{1}{\rho}\frac{\partial}{\partial\rho}+\frac{\partial^2}{\partial\rho^2}.\end{aligned} \tag{3.20}$$

Substituting (3.13), (3.19) and (3.20) into (3.12), we obtain

$$\begin{aligned}\Big(\vec{\nabla}^2_{\vec{r}_1}+\vec{\nabla}^2_{\vec{r}_2}\Big) &= \frac{1}{\rho}\frac{\partial}{\partial\rho}+\frac{\partial^2}{\partial\rho^2}+\frac{1}{\rho^2}\frac{\partial^2}{\partial\alpha^2}+\frac{4}{\rho}\frac{\partial}{\partial\rho}+\frac{4}{\rho^2}\cot 2\alpha\frac{\partial}{\partial\alpha}\\ &\quad -\frac{\vec{\ell}^2_{\vec{r}_1}}{\rho^2\cos^2\alpha}-\frac{\vec{\ell}^2_{\vec{r}_2}}{\rho^2\sin^2\alpha}\\ &= \frac{\partial^2}{\partial\rho^2}+\frac{5}{\rho}\frac{\partial}{\partial\rho}-\frac{1}{\rho^2}\Big(-\frac{\partial^2}{\partial\alpha^2}-4\cot 2\alpha\frac{\partial}{\partial\alpha}\\ &\quad -\frac{\vec{\ell}^2_{\vec{r}_1}}{\cos^2\alpha}-\frac{\vec{\ell}^2_{\vec{r}_2}}{\sin^2\alpha}\Big)\\ &= \frac{\partial^2}{\partial\rho^2}+\frac{5}{\rho}\frac{\partial}{\partial\rho}-\frac{1}{\rho^2}\hat{K}^2,\end{aligned} \tag{3.21}$$

University of South Africa ETD Grobler, J. (2010)

where,

$$\hat{K}^2 = \Big(-\frac{\partial^2}{\partial\alpha^2} - 4\cot(2\alpha)\frac{\partial}{\partial\alpha} + \frac{\vec{\ell}^2_{\vec{r}_1}}{\cos^2\alpha} + \frac{\vec{\ell}^2_{\vec{r}_2}}{\sin^2\alpha}\Big). \tag{3.22}$$

The operator $\hat{K}^2$, and the associated eigenfunctions, are covered in the theory of hyperspherical harmonics [25]. The operator $\hat{K}^2$ absorbs all the angular variables. The solutions of the eigenvalue problem

$$\hat{K}^2\phi_{[L]}(\omega) = L(L+4)\phi_{[L]}(\omega), \tag{3.23}$$

are the so-called hyperspherical harmonics which depend on the set of hyperangles

$$\omega = \{\Omega_{\vec{r}_1}, \Omega_{\vec{r}_2}, \alpha\}.$$

The subscript $[L]$ in (3.23) is the multi-index

$$[L] = \{L, \ell_1, \ell_2, m_1, m_2\}, \tag{3.24}$$

which includes the grand orbital quantum number,

$$L = \ell_1 + \ell_2 + 2n, \qquad n = 0, 1, 2\ldots. \tag{3.25}$$

The function $\phi_{[L]}(\omega)$ introduced in (3.23) is of the form

$$\phi_{[L]}(\omega) = K_L^{\ell_1\ell_2 m_1 m_2}(\omega)\chi_{[s]}, \tag{3.26}$$

where, the factor

$$K_L^{\ell_1\ell_2 m_1 m_2}(\omega) = N_L^{\ell_1\ell_2}(\cos\alpha)^{\ell_1}(\sin\alpha)^{\ell_2}P^{\ell_2+\frac{1}{2},\ell_1+\frac{1}{2}}(\cos 2\alpha)Y_{\ell_1 m_1}Y_{\ell_2 m_2}, \tag{3.27}$$

contains the hyperangular components [19].

The factor $\chi_{[s]}$ is the three-body spin state vector, with $[s] = ((s_1 s_2)s_{12}s_3)s\sigma$. Subscripts 1, 2 and 3 represent the spins of the two Λ-particles and the nucleus, respectively. The term s represents the three-body spin and $P^{\ell_2+\frac{1}{2},\ell_1+\frac{1}{2}}$

University of South Africa ETD Grobler, J. (2010)

is the spin permutation operator (also written in the form P^{σ}), which acts in the spin space.

The factor $N_L^{\ell_1\ell_2}$ has the form

$$N_L^{\ell_1\ell_2} = \sqrt{\frac{2n!(L+2)(n+\ell_1+\ell_2+1)!}{\Gamma(n+\ell_1+\frac{3}{2})\Gamma(n+\ell_2+\frac{3}{2})}}. \tag{3.28}$$

Substituting (3.21) into (3.5), we obtain

$$\begin{aligned} H &= -\frac{\hbar^2}{2m_\Lambda}\Big(\frac{\partial^2}{\partial\rho^2}+\frac{5}{\rho}\frac{\partial}{\partial\rho}-\frac{1}{\rho^2}\hat{K}^2\Big)+V_{\Lambda\Lambda}(\mid \vec{r}_1-\vec{r}_2 \mid)+V_1(r_1)+V_2(r_2) \\ &= H_o+V_{\Lambda\Lambda}(\mid \vec{r}_1-\vec{r}_2 \mid)+V_1(r_1)+V_2(r_2), \end{aligned}$$

where

$$H_o = -\frac{\hbar^2}{2m_\Lambda}\Big(\frac{\partial^2}{\partial\rho^2}+\frac{5}{\rho}\frac{\partial}{\partial\rho}-\frac{1}{\rho^2}\hat{K}^2\Big). \tag{3.29}$$

Hence, the Hamiltonian for the system is

$$H = H_o + V_{\Lambda\Lambda} + V_1 + V_2, \tag{3.30}$$

where H_o is of the form (3.29).

3.3.1 Volume Element

The volume element in the hyperspherical coordinate system is

$$d\vec{r}_1\, d\vec{r}_2 = r_1^2 r_2^2 \sin\theta_{\vec{r}_1}\sin\theta_{\vec{r}_2}\, dr_1\, dr_2\, d\theta_{\vec{r}_1}\, d\theta_{\vec{r}_2}\, d\varphi_{\vec{r}_1}\, d\varphi_{\vec{r}_2}. \tag{3.31}$$

In polar coordinates, we have

$$dr_1\, dr_2 = \rho\, d\rho\, d\alpha, \tag{3.32}$$

and substituting (3.3) and (3.32) into (3.31), we obtain

$$d\vec{r}_1\, d\vec{r}_2 = (\rho^2\cos^2\alpha)(\rho^2\sin^2\alpha)\sin\theta_{\vec{r}_1}\sin\theta_{\vec{r}_2}\rho\, d\rho\, d\alpha\, d\theta_{\vec{r}_1}\, d\theta_{\vec{r}_2}\, d\varphi_{\vec{r}_1}\, d\varphi_{\vec{r}_2}$$

University of South Africa ETD Grobler, J. (2010)

$$
\begin{aligned}
&= (\rho^5 d\rho)(\sin^2\alpha\cos^2\alpha\rho^2 d\alpha)(\sin\theta_{\vec{r}_1} d\theta_{\vec{r}_1} d\varphi_{\vec{r}_1})(\sin\theta_{\vec{r}_2}\, d\theta_{\vec{r}_2}\, d\varphi_{\vec{r}_2}) \\
&= (\rho^5\, d\rho)(\sin^2\alpha\cos^2\alpha\rho^2\, d\alpha)\, d\Omega_{\vec{r}_1}\, d\Omega_{\vec{r}_2} \\
&= \rho^5\, d\rho\, d\omega,
\end{aligned}
$$

where

$$
d\omega = \frac{1}{4}\sin^2 2\alpha\, d\alpha\, d\Omega_{\vec{r}_1}\, d\Omega_{\vec{r}_1}, \tag{3.33}
$$

and

$$
d\Omega_{\vec{r}_1} = \sin\theta_{\vec{r}_1}\, d\theta_{\vec{r}_1}\, d\varphi_{\vec{r}_2},
$$

which is defined as the spherical angle. Integrating (3.33) over the interval $0 \leq \alpha \leq \pi/2$, we obtain the volume element in the hyperspherical coordinate system,

$$
\begin{aligned}
\int_0^{\frac{\pi}{2}} d\omega &= \int_0^{\frac{\pi}{2}} \frac{1}{4}\sin^2\alpha\, d\alpha\, d\Omega_{\vec{r}_1}\, d\Omega_{\vec{r}_2} \\
&= \int_0^{\frac{\pi}{2}} \frac{1}{4}\sin^2\alpha\, d\alpha \left(\int_0^{\pi} \sin\theta_{\vec{r}_1}\, d\theta_{\vec{r}_1} \int_0^{2\pi} d\varphi_{\vec{r}_1}\right)\left(\int_0^{\pi} \sin\theta_{\vec{r}_2} d\theta_{\vec{r}_2} \int_0^{2\pi} d\varphi_{\vec{r}_2}\right) \\
&= 16\pi^2 \int_0^{\frac{\pi}{2}} \frac{1}{4}\sin^2\alpha\, d\alpha \\
&= 16\pi^2\left(\frac{1}{8}\int_0^{\frac{\pi}{2}} d\alpha - \frac{1}{2}\int_0^{\frac{\pi}{2}} \cos 4\alpha\, d\alpha\right) \\
&= 16\pi^2\left(\frac{\pi}{16}\right) \\
&= \pi^3.
\end{aligned} \tag{3.34}
$$

University of South Africa ETD Grobler, J. (2010)

3.4 Schrödinger Equation of the System

The central-force problem proposed in our system enables the reduction of the six-dimensional Schrödinger Equation of the form

$$H\psi(\vec{r}_1,\vec{r}_2) = E\psi(\vec{r}_1,\vec{r}_2). \tag{3.35}$$

In order to derive the Schrödinger Equation for the system, we use an approach similar to the two-body partial wave decomposition [25], where a two-body wave function of the form

$$\psi(\vec{r}_1,\vec{r}_2) = \frac{1}{\rho^{\frac{5}{2}}}\sum_{[L]} u_{[L]}(\rho)\phi_{[L]}(\omega), \tag{3.36}$$

is employed and the hyperradial and angular components are included in the terms $u_{[L]}$ and $\phi_{[L]}(\omega)$, respectively. The coefficient $1/\rho^{\frac{5}{2}}$ is introduced in order to eliminate the first-order derivative in the hyperradial Schrödinger Equation. The hyperangle, ω, is related to the pair $(\vec{r}_1,\vec{r}_2)$.

Substituting (3.30) and (3.36) into (3.35), we obtain for the first term

$$\left[-\frac{\hbar^2}{2m_\Lambda}\left(\frac{\partial^2}{\partial\rho^2}+\frac{5}{\rho}\frac{\partial}{\partial\rho}-\frac{1}{\rho^2}\hat{K}^2\right)+V_{\Lambda\Lambda}(\mid\vec{r}_1-\vec{r}_2\mid)+V_1(r_1)+V_2(r_2)\right]$$
$$\times\left(\frac{1}{\rho^{\frac{5}{2}}}\sum_{[L]}u_{[L]}(\rho)\phi_{[L]}(\omega)\right) = E\left(\frac{1}{\rho^{\frac{5}{2}}}\sum_{[L]}u_{[L]}(\rho)\phi_{[L]}(\omega)\right). \tag{3.37}$$

Evaluating the first two terms in parenthesis on the left-hand side of (3.37), we obtain, for the first term

$$\frac{\partial^2}{\partial\rho^2}\left(\frac{1}{\rho^{\frac{5}{2}}}\sum_{[L]}u_{[L]}(\rho)\phi_{[L]}(\omega)\right) = \frac{\partial}{\partial\rho}\left[\frac{\partial}{\partial\rho}\left(\frac{1}{\rho^{\frac{5}{2}}}\sum_{[L]}u_{[L]}(\rho)\phi_{[L]}(\omega)\right)\right]$$

$$= \frac{\partial}{\partial\rho}\left[\left(\sum_{[L]}u_{[L]}(\rho)\phi_{[L]}(\omega)\right)\frac{\partial}{\partial\rho}\left(\frac{1}{\rho^{\frac{5}{2}}}\right)+\frac{1}{\rho^{\frac{5}{2}}}\frac{\partial}{\partial\rho}\left(\sum_{[L]}u_{[L]}(\rho)\phi_{[L]}(\omega)\right)\right]$$

University of South Africa ETD Grobler, J. (2010)

$$= \frac{\partial}{\partial\rho}\Big[-\frac{5}{2\rho^{\frac{7}{2}}}\Big(\sum_{[L]}u_{[L]}(\rho)\phi_{[L]}(\omega)\Big)+\frac{1}{\rho^{\frac{5}{2}}}\Big(\sum_{[L]}u'_{[L]}(\rho)\phi_{[L]}(\omega)\Big)\Big]$$

$$= \frac{35}{4\rho^{\frac{9}{2}}}\Big(\sum_{[L]}u_{[L]}(\rho)\phi_{[L]}(\omega)\Big)-\frac{5}{2\rho^{\frac{7}{2}}}\Big(\sum_{[L]}u'_{[L]}(\rho)\phi_{[L]}(\omega)\Big)$$

$$-\frac{5}{2\rho^{\frac{7}{2}}}\Big(\sum_{[L]}u'_{[L]}(\rho)\phi_{[L]}(\omega)\Big)+\frac{1}{\rho^{\frac{5}{2}}}\Big(\sum_{[L]}u''_{[L]}(\rho)\phi_{[L]}(\omega)\Big), \tag{3.38}$$

and, for the second term

$$\frac{5}{\rho}\frac{\partial}{\partial\rho}\Big(\frac{1}{\rho^{\frac{5}{2}}}\sum_{[L]}u_{[L]}(\rho)\phi_{[L]}(\omega)\Big)=\Big[\frac{5}{\rho}\Big(\sum_{[L]}u_{[L]}(\rho)\phi_{[L]}(\omega)\Big)\frac{\partial}{\partial\rho}\Big(\frac{1}{\partial^{\frac{5}{2}}}\Big)\Big]$$

$$+\Big[\frac{5}{\rho}\frac{1}{\rho^{\frac{5}{2}}}\frac{\partial}{\partial\rho}\Big(\sum_{[L]}u_{[L]}(\rho)\phi_{[L]}(\omega)\Big)\Big]$$

$$=-\frac{25}{9\rho^{\frac{9}{2}}}\Big(\sum_{[L]}u_{[L]}(\rho)\phi_{[L]}(\omega)\Big)+\frac{5}{\rho^{\frac{7}{2}}}\Big(\sum_{[L]}u'_{[L]}(\rho)\phi_{[L]}(\omega)\Big). \tag{3.39}$$

Substituting (3.38) and (3.39) into (3.29), we obtain,

$$H_o\psi(\vec{r}_1\vec{r}_2)=-\frac{\hbar^2}{2m_\Lambda}\Big(\frac{\partial^2}{\partial\rho^2}+\frac{5}{\rho}\frac{\partial}{\partial\rho}-\frac{1}{\rho^2}\hat{K}^2\Big)\Big(\frac{1}{\rho^{\frac{5}{2}}}\sum_{[L]}u_{[L]}(\rho)\phi_{[L]}(\omega)\Big)$$

$$= -\frac{\hbar^2}{2m_\Lambda}\Big[\Big(\frac{35}{4\rho^{\frac{9}{2}}}\sum_{[L]}u_{[L]}(\rho)\phi_{[L]}(\omega)\Big)+\frac{1}{\rho^{\frac{5}{2}}}\Big(\sum_{[L]}u''_{[L]}(\rho)\phi_{[L]}(\omega)\Big)$$

$$-\frac{1}{\rho^{\frac{5}{2}}}\Big(\sum_{[L]}u_{[L]}(\rho)\phi_{[L]}(\omega)\Big)-\frac{1}{\partial^2}\frac{1}{\rho^{\frac{5}{2}}}\hat{K}^2\Big(\sum_{[L]}u_{[L]}(\rho)\phi_{[L]}(\omega)\Big)\Big]$$

$$= -\frac{\hbar^2}{2m_\Lambda}\sum_{[L]}u_{[L]}\Big[\frac{35}{4\rho^{\frac{9}{2}}}u_{[L]}(\rho)\phi_{[L]}(\omega)+\frac{1}{\rho^{\frac{5}{2}}}u''_{[L]}(\rho)\phi_{[L]}(\omega)-$$

$$\frac{25}{2\rho^{\frac{9}{2}}}u_{[L]}(\rho)\phi_{[L]}(\omega)-\frac{1}{2\rho^{\frac{9}{2}}}u_{[L]}L(L+4)(\rho)\phi_{[L]}(\omega)\Big]$$

$$= -\frac{\hbar^2}{2m_\Lambda}\sum_{[L]}\Big[\frac{1}{\rho^{\frac{5}{2}}}u_{[L]}(\rho)\phi_{[L]}(\omega)+\frac{15}{2\rho^{\frac{9}{2}}}u_{[L]}(\rho)\phi_{[L]}(\omega)-$$

University of South Africa ETD Grobler, J. (2010)

$$\frac{1}{\rho^{\frac{9}{2}}}u_{[L]}L(L+4)(\rho)\phi_{[L]}(\omega)\Big]$$

$$= -\frac{\hbar^2}{2m_\Lambda}\sum_{[L]}\left[\frac{1}{\rho^{\frac{5}{2}}}u''_{[L]}(\rho)\phi_{[L]}(\omega) - \left(\frac{L(L+4)+\frac{15}{4}}{\rho^{\frac{9}{2}}}\right)u_{[L]}(\rho)\right]\phi_{[L]}(\omega) \quad (3.40)$$

Substituting (3.40) into (3.37), we obtain the following eigenvalue equation

$$\begin{aligned} H\psi(\vec{r}_1,\vec{r}_2) &= -\frac{\hbar^2}{2m_\Lambda}\sum_{[L]}\left[\frac{1}{\rho^{\frac{5}{2}}}u''_{[L]}(\rho)\phi_{[L]}(\omega) - \left(\frac{L(L+4)+\frac{15}{4}}{\rho^{\frac{9}{2}}}\right)u_{[L]}(\rho)\right]\phi_{[L]}(\omega) \\ &= \left[V_{\Lambda\Lambda}(\mid \vec{r}_1-\vec{r}_2 \mid) + V_1(r_1) + V_2(r_2)\right]\frac{1}{\rho^{\frac{5}{2}}}\sum_{[L]}u_{[L]}(\rho)\phi_{[L]}(\omega) \\ &= E\frac{1}{\rho^{\frac{5}{2}}}\sum_{[L]}u_{[L]}(\rho)\phi_{[L]}(\omega). \end{aligned} \quad (3.41)$$

Next, we multiply (3.41) on the left-hand side by

$$-\frac{2m_\Lambda}{\hbar^2}\rho^{\frac{5}{2}}\phi^*_{[L]}(\omega),$$

("$*$" represents the complex conjugate) and then integrate with respect to ω over all the angular variables, giving

$$-\frac{\hbar^2}{2m_\Lambda}\frac{2m_\Lambda\rho^{\frac{5}{2}}}{\hbar^2}\int\sum_{[L]}\left[\frac{1}{\rho^{\frac{5}{2}}}u''_{[L]}(\rho)\phi_{[L]}(\omega) - \left(\frac{L(L+4)+\frac{15}{4}}{\rho^{\frac{9}{2}}}\right)u_{[L]}(\rho)\right]\phi^*_{[L]}(\omega)\phi_{[L']}(\omega)\,d\omega$$

$$+\frac{2m_\Lambda\rho^{\frac{5}{2]}}}{\hbar^2}\frac{1}{\rho^{\frac{5}{2}}}\int\left[V_{\Lambda\Lambda}(\mid \vec{r}_1-\vec{r}_2 \mid) + V_1(r_1) + V_2(r_2)\right]\sum_{[L]}u_{[L]}(\rho)\phi^*_{[L]}(\omega)\phi_{[L']}(\omega)\,d\omega$$

$$= E\frac{2m_\Lambda\rho^{\frac{5}{2}}}{\hbar^2}\left[\frac{1}{\rho^{\frac{5}{2}}}\int\sum_{[L]}u_{[L]}(\rho)\phi^*_{[L]}(\omega)\phi_{[L']}(\omega)\,d\omega\right]$$

$$\left[u''_{[L]}(\rho) - \left(\frac{L(L+4)+\frac{15}{4}}{\rho^2}\right)\right]u_{[L]}(\rho) + \sum_{[L]}\frac{2m_\Lambda}{\hbar^2}\Big[\int\left(V_{\Lambda\Lambda}(\mid \vec{r}_1-\vec{r}_2 \mid) + V_1(r_1) + V_2(r_2)\right)$$

$$\times\phi^*_{[L]}(\omega)\phi_{[L']}(\omega)\,d\omega\Big]u_{[L']}(\rho) = \frac{2m_\Lambda E}{\hbar^2}u_{[L]}(\rho).$$

University of South Africa ETD Grobler, J. (2010)

Hence, we obtain the following system of hyperradial equations

$$\left[\frac{\partial^2}{\partial\rho^2} + k^2 - \frac{L(L+4)+\frac{15}{4}}{\rho^2}\right] u_{[L]}(\rho) = \sum_{[L]} V_{[L][L']}(\rho) u_{[L']}(\rho), \tag{3.42}$$

where $V_{[L][L']}$ is a potential matrix of the form

$$V_{[L][L']} = \frac{2m_\Lambda}{\hbar^2} \int \phi^*_{[L]}(\omega)\Big[V_{\Lambda\Lambda}(\mid \vec{r}_1 - \vec{r}_2 \mid) + V_1(r_1) + V_2(r_2)\Big]\phi_{[L']}(\omega)\, d\omega.$$

Introducing the parameter λ and substituting this into (3.42), where

$$\lambda = L + \frac{3}{2}, \tag{3.43}$$

and noting that

$$\begin{aligned} L(L+4) + \frac{15}{4} &= \left(L + \frac{3}{2}\right)\left(L + \frac{5}{2}\right) \\ &= \lambda(\lambda+1), \end{aligned}$$

we obtain the desired result, the set of hyperradial Schrödinger Equations for the system

$$\left[\frac{\partial^2}{\partial\rho^2} + k^2 - \frac{\lambda(\lambda+1)}{\rho^2}\right] u_{[L]}(k,\rho) = \sum_{[L']} V_{[L][L']}(\rho) u_{[L']}(k,\rho), \tag{3.44}$$

where k, the hypermomentum, is given by

$$k^2 = \frac{2m_\Lambda E}{\hbar^2},$$

where use has been made of the orthonormality relation of hyperspherical harmonics

$$\int \phi^*_{[L]}(\omega)\phi_{[L']}(\omega)\, d\omega = \delta_{[L]}\delta_{[L']},$$

and the relation [21]

$$\chi^\dagger_{[s]}\chi_{[s]} = 1.$$

University of South Africa ETD Grobler, J. (2010)

Chapter 4

Method of Solution

4.1 The Jost Function

We consider the general form of the radial Schrödinger Equation [21]

$$\left[\frac{\partial^2}{\partial r^2} + k^2 - \frac{l(l+1)}{r^2} - V(r)\right] u_l(k,r) = 0, \tag{4.1}$$

where $k^2 = 2mE/\hbar^2$, l is the angular momentum quantum number, $u_l(k,r)$ is the radial wave function, and r is the radius.

The boundary conditions for the physical solutions of (4.1) are imposed at both ends of the interval $r \in [0,\infty)$. Regularity of the wave function at the origin requires that

$$u_l(k,0) = 0, \tag{4.2}$$

a condition which exists for all solutions. However, the conditions for $r \to \infty$ are different for bound, scattering and resonant states. If the potential $V(r)$ vanishes at large distances faster than $1/r^2$, then (4.1) takes the form of the "free" radial Schrödinger Equation [26],

$$\left[\frac{\partial^2}{\partial r^2} + k^2 - \frac{l(l+1)}{r^2}\right] u_l(k,r) = 0. \tag{4.3}$$

University of South Africa ETD Grobler, J. (2010)

This equation has two linearly independent solutions, namely, the Riccati-Hankel functions $h_l^{(-)}(kr)$ and $h_l^{(+)}(kr)$ [27], which behave as

$$h_l^{(\pm)}(kr) \underset{r\to\infty}{\longrightarrow} \mp i \exp[\pm i(kr - l\pi/2)]. \tag{4.4}$$

The general asymptotic form of the wavefunction can be constructed from a linear combination of these Riccati-Hankel functions,

$$u_l(k,r) \underset{r\to\infty}{\longrightarrow} C_1 h_l^{(-)}(kr) + C_2 h_l^{(+)}(kr), \tag{4.5}$$

where appropriate choice of the combination coefficients C_1 and C_2 determine the type of physical solutions. These coefficients are functions of the total energy of the system and the angular momentum. The radial wavefunction $u_l(k,r)$ can be written in terms of the asymptotics of (4.4) as

$$u_l(k,r) \underset{r\to\infty}{\longrightarrow} h_l^{(-)}(kr) f_l^{(-)}(k) + h_l^{(+)}(kr) f_l^{(+)}(k), \tag{4.6}$$

where $C_1 = f_l^{(-)}(k)$ and $C_2 = f_l^{(+)}(k)$. The energy-dependent amplitudes $f_l^{(\pm)}(k)$ of the incoming and outgoing waves are called the Jost functions [26].

For bound states, the wave function (4.6) must vanish at large distances

$$u_l(k_n,r) \underset{r\to\infty}{\longrightarrow} 0. \tag{4.7}$$

The total energy for a bound state is negative and the momentum is pure imaginary

$$k_n = \sqrt{-2m|E_n|/\hbar^2} = i\kappa_n, \qquad \kappa_n > 0. \tag{4.8}$$

Substituting (4.8) into (4.4), we find that one of the two asymptotic terms of (4.4) grows exponentially, while the other vanishes exponentially

$$h_l^{(\pm)}(kr) \underset{r\to\infty}{\sim} \exp(\mp\kappa r). \tag{4.9}$$

University of South Africa ETD Grobler, J. (2010)

Therefore, only the second term in (4.6) can survive in the bound state wave function,

$$u_l(k_n, r) \underset{r\to\infty}{\longrightarrow} h_l^{(+)}(k_n r) f_l^{(+)}(k_n). \tag{4.10}$$

This may be achieved for certain points such that

$$f_l^{(-)}(k_n) = 0. \tag{4.11}$$

Therefore, bound states correspond to positive imaginary zeros of the Jost function.

The Jost function is a complex function of the total energy of the quantum state, which may be real or complex. The most useful property of the Jost function is that it is an analytic function for all complex energies and has simple zeros for bound states. It seems therefore logical to approach a solution to our model by using a method to determine the Jost function as we could then determine the bound states.

4.2 Three-body Jost Matrix

The Jost function for the single-channel case were covered in the previous section. As our hypernuclear system is a three-body problem, we recast the formalism of the previous section for the multi-channel case.

A method for calculating the Jost function for analytic potential were developed, and successfully applied to hypernuclear systems [19, 28, 29]. The method uses a combination of the hyperspherical approach, complex rotation and the properties of the Jost function in order to determine bound states.

University of South Africa ETD Grobler, J. (2010)

The physical solutions of (3.44) are defined by the boundary condition requirement

$$u_{[L]}(k,\rho) \underset{\rho\to 0}{\longrightarrow} 0, \tag{4.12}$$

and, at infinity must be of the form

$$u_{[L]}(k,\rho) \underset{\rho\to \infty}{\longrightarrow} U_{[L]}(k,\rho), \tag{4.13}$$

where $U_{[L]}(k,\rho)$ has terms describing the open channels.

We follow the methods set out in [19, 28, 29] and consider (3.44) as a matrix equation with each of its solutions forming a column matrix. According to the general theory of differential equations, there are as many independent regular column-solutions as there are equations in the system [30],

$$\left[\frac{\partial^2}{\partial\rho^2} + k^2 - \frac{\lambda(\lambda+1)}{\rho^2}\right]\Phi_{[L][L']}(k,\rho) = \sum_{[L'']} V_{[L][L'']}(\rho)\Phi_{[L][L'']}(k,\rho), \tag{4.14}$$

where

$$\Phi_{[L][L']}(k,\rho) = \frac{1}{2}\Big[h_\lambda^{(-)}(k\rho)F^{(-)}_{[L][L']}(k,\rho) + h_\lambda^{(+)}(k\rho)F^{(+)}_{[L][L']}(k,\rho)\Big], \tag{4.15}$$

and $h_\lambda^{(\pm)}(k\rho)$ are the Riccati-Hankel functions [27]. The inclusion of the Riccati-Hankel in the construction of the regular basis ensures the correct asymptotic behaviour of the basic solutions at large ρ.

The two terms $||F^{(\pm)}_{[L][L']}(k,\rho)||$ in (4.15) are unknown matrices, introduced in order for the construction of different physical solutions. Since according to (4.12), all physical solutions must be regular at $\rho = 0$, any one of them is a linear combination of the regular column-solutions. As we seek to determine these two unknown matrices, reason dictates [30] that we need two equations. We obtain these equations by making use of the Lagrange condition

$$h_\lambda^{(-)}(k\rho)F^{(-)}_{[L][L']}(k,\rho) + h_\lambda^{(+)}(k\rho)F^{(+)}_{[L][L']}(k,\rho) = 0. \tag{4.16}$$

University of South Africa ETD Grobler, J. (2010)

Substituting (4.15) into the hyperradial equation (4.14) and using the condition (4.16), we obtain the following system of first-order coupled differential equations for the unknown matrices $F^{(\pm)}_{[L][L']}(k,\rho)$,

$$\begin{cases} \partial_\rho F^{(-)}_{[L][L']}(k,\rho) &= -\dfrac{h^{(+)}_\lambda(k\rho)}{2ik}\displaystyle\sum_{[L'']} V_{[L][L'']}(\rho)\Big[h^{(-)}_{\lambda''}(k\rho)F^{(-)}_{[L''][L']}(k,\rho), \\ & \quad +h^{(+)}_\lambda(k\rho)F^{(+)}_{[L''][L]}(k,\rho)\Big], \\ \partial_\rho F^{(+)}_{[L][L']}(k,\rho) &= \dfrac{h^{(-)}_\lambda(k\rho)}{2ik}\displaystyle\sum_{[L'']} V_{[L][L'']}(\rho)\Big[h^{(-)}_{\lambda''}(k\rho)F^{(-)}_{[L''][L']}(k,\rho), \\ & \quad +h^{(+)}_\lambda(k\rho)F^{(+)}_{[L''][L]}(k,\rho)\Big], \end{cases} \tag{4.17}$$

which are equivalent to (3.44). These equations are convenient for solving our model.

The equations (4.17) require suitable boundary conditions at $\rho = 0$. It can be shown [31] that for a three-body system, the coupled hyperradial Schrödinger Equations (4.17) have a system of linearly independent, regular column solutions which vanish near $\rho = 0$ such that

$$\lim_{\rho\to 0}\frac{\Phi_{[L][L']}(k,\rho)}{\rho^{\lambda'+1}} = \delta_{[L][L']}. \tag{4.18}$$

To ensure consistency with the definition of the regular solution, we define a regular basis using the boundary condition [31]

$$\lim_{\rho\to 0}\frac{\Phi_{[L][L']}(k,\rho)}{j_{\lambda'}(k\rho)} = \delta_{[L][L']}, \tag{4.19}$$

where $j_{\lambda'}(k\rho)$ is the Riccati-Bessel function [27], in accordance with the corresponding definition of the three-body problem.

As $\Phi_{[L][L']}(k,\rho)$ is regular at $\rho = 0$, we can expect that the functions $F^{(\pm)}_{[L][L']}(k,\rho)$ of (4.15) near the origin ensure that the singularities of $h^{(\pm)}_\lambda(k\rho)$ compensate

University of South Africa ETD Grobler, J. (2010)

each other. Such a condition is achieved [31] if the functions $F^{(\pm)}_{[L][L']}(k\rho)$ are identical as $\rho \to 0$, or

$$F^{(\pm)}_{[L][L']}(k,\rho) \underset{\rho\to 0}{\sim} F_{[L][L']}(k,\rho), \tag{4.20}$$

as then

$$\Phi_{[L][L']}(k,\rho) \underset{\rho\to 0}{\sim} j_\lambda(k\rho) F_{[L][L']}(k,\rho), \tag{4.21}$$

so that the boundary conditions (4.19) then become

$$\lim_{\rho\to 0}\left[\frac{j_\lambda(k\rho)F_{[L][L']}(k,\rho)}{j_{\lambda'}(k\rho)}\right] = \delta_{[L][L']}. \tag{4.22}$$

However, $\rho = 0$ is a singular point as the Riccati-Hankel functions have the short-range behaviour $\approx \rho^{-L}$. Therefore, Eqs. (4.17) cannot be solved numerically with the boundary conditions at $\rho = 0$. We may [29], however, use analytical solutions (in the form of a series expansion) of (4.17) in the small interval $(0, \delta]$, imposing the boundary conditions at $\rho = \delta$

$$F^{(\pm)}_{[L][L']}(k,\delta) \approx F^{(N)}_{[L][L']}(k,\delta). \tag{4.23}$$

The right hand side of (4.17) vanishes when $\rho \to \infty$ [31]. The derivatives of (4.17) also vanish, therefore the functions $F^{(\pm)}_{[L][L']}(k,\rho)$ become ρ-independent. Hence, we have

$$\Phi_{[L][L']}(k,\rho) \underset{\rho\to\infty}{\sim} \frac{1}{2}\Big[h^{(-)}_\lambda(k\rho) f^{(-)}_{[L][L']}(k) + h^{(+)}_\lambda(k\rho) f^{(+)}_{[L][L']}(k)\Big], \tag{4.24}$$

where

$$f^{(\pm)}_{[L][L']}(k) = \lim_{\rho\to\infty} F^{(\pm)}_{[L][L']}(k,\rho). \tag{4.25}$$

There ρ-independent matrices $||f^{(\pm)}_{[L][L']}||$ are termed the *Jost matrices*.

The Jost matrices can be used to determine the asymptotic behaviour of the fundamental system of regular solutions (4.17).

University of South Africa ETD Grobler, J. (2010)

For complex values of k, the limits (4.25) exist in different domains of the complex plane, namely, $f^{(+)}_{[L][L']}(k)$ in the lower half and $f^{(-)}_{[L][L']}(k)$ in the upper half. For a particular class of potentials, the upper bound for the existence of $f^{(+)}_{[L][L']}(k)$ is shifted upwards and the lower bound for $f^{(-)}_{[L][L']}(k)$ is shifted downwards, thereby widening their common area. Difficulties concerning the existence of the limits (4.25) can be circumvented by using the complex rotation method which is discussed in the sections that follow.

4.3 Method of Locating Bound States

In the theory of quantum mechanics [32], a bound state is characterized by wave functions which vanish at large distances. This is because the probability of locating a bound particle at large distances from the bound region must decrease with increasing distance from that region. The probability is directly dependent on the modulus of the wave function,

$$\psi(r) \underset{\rho\to\infty}{\longrightarrow} 0.$$

The deuteron is an example of a bound state of the proton and the neutron. The binding energy of the deuteron is 2.22 MeV and is the only bound state of two nucleons [2]. The bound state of the deuteron may exist indefinitely.

Bound states occur at negative energies, where the potentials describing such behaviour are negative, thereby having a "pulling-in" effect. An example of such a potential is the optical potential [21].

The bound state wave function, at large distances, can be written as

$$\sum_{[L']} \Phi_{[L][L']}(k,\rho) C_{[L']} \underset{\rho\to\infty}{\longrightarrow} 0. \tag{4.26}$$

University of South Africa ETD Grobler, J. (2010)

Here, the function $\Phi_{[L][L']}(k,\rho)$ can be replaced by its asymptotic form

$$\frac{1}{2}\sum_{[L']}[h_\lambda^{(+)}(k\rho)f^{(+)}_{[L][L']}(k)+h_\lambda^{(-)}(k\rho)f^{(-)}_{[L][L']}(k)]C_{[L']}\underset{\rho\to\infty}{\longrightarrow}0. \tag{4.27}$$

The total energy for a bound state is negative with the corresponding momentum being pure imaginary. Due to the properties of the Riccati-Hankel functions, with increasing distances from the origin, the term $h_\lambda^{(-)}(k\rho)$ of (4.27) grows exponentially while the other term $h_\lambda^{(+)}(k\rho)$ decays exponentially. Hence, the condition (4.27) can only be achieved if we find combination coefficients $C_{[L']}$ such that the diverging functions $h_\lambda^{(-)}(k\rho)$ of different columns cancel out, giving

$$\sum_{[L']} f^{(-)}_{[L][L']}(k)C_{[L']}=0. \tag{4.28}$$

Bound states are the points at which the physical solution consists of only outgoing waves in its asymptotics.

The system of homogenous linear equations has a non-trivial solution provided that

$$\det||f^{(-)}(k)||=0. \tag{4.29}$$

The condition (4.29) enables us to determine all possible bound states by looking for zeros of the Jost matrix determinant on the positive imaginary axis. For each zero found, the coefficients $C_{[L]}$ are then uniquely determined by the system (4.28) apart from a general normalization factor. The normalization factor is fixed when the physical wavefunction is normalized.

4.4 Minimal Approximation

The Schrödinger Equation (3.44) is of the same form as the radial coupled-channels Schrödinger equation [32] and includes the centrifugal potential

University of South Africa ETD Grobler, J. (2010)

term $\lambda(\lambda+1)/\rho^2$. These similarities enable the Schrödinger Equation (3.44) to be solved using the Jost function method [19, 28, 29].

However, the system (3.44) consists of an infinite number of equations and in order to make it of any practical use, we have to truncate it somewhere. In order to achieve this, we employ the minimal approximation method.

In the minimal approximation we retain only the first term in (3.36), giving

$$\psi(\vec{r}_1,\vec{r}_2) \approx \frac{1}{\rho^{\frac{5}{2}}} u_{[L_{min}]}(\rho)\phi_{[L_{min}]}(\omega),$$

and we assume the minimal value of the grand orbital angular momentum, $n=0$, called the hypercentral approximation. In this approximation, (3.24) becomes $[L]=[L_{min}]$, with $L=L_{min}=0$, giving

$$\lambda = \lambda_{min} = \frac{3}{2},$$

and

$$\left[\frac{\partial^2}{\partial\rho^2} + k^2 - \frac{\lambda_{min}(\lambda_{min}+1)}{\rho^2}\right] u_{[0]}(k,\rho) = \langle U\rangle u_{[0]}(k,\rho),$$

where

$$\langle U\rangle = \frac{2m_\Lambda}{\hbar^2}\int \phi^*_{[0]}(\omega)\Big[V_{\Lambda\Lambda}(\mid \vec{r}_1-\vec{r}_2\mid) + V_1(r_1) + V_2(r_2)\Big]\phi_{[0]}(\omega)\,d\omega. \quad (4.30)$$

For the case $\ell_1=\ell_2=L_{min}=0$, we have

$$N_0^{00} = \frac{4}{\sqrt{\pi}}, \quad (4.31)$$

$$P^{\frac{1}{2}\frac{1}{2}} = 1, \quad (4.32)$$

and,

$$K_0^{0000} = \pi^{-3/2}. \quad (4.33)$$

University of South Africa ETD Grobler, J. (2010)

Hence, (3.26) takes the form

$$\phi_{[0]} = \pi^{-\frac{3}{2}}. \tag{4.34}$$

Substituting (4.34) into (4.30), we obtain the hypercentral potential for our hypernuclear system

$$\langle U \rangle = \frac{2m_\Lambda}{\pi^3 \hbar^2} \int \Big[V_{\Lambda\Lambda}(\mid \vec{r}_1 - \vec{r}_2 \mid) + V_1(r_1) + V_2(r_2) \Big] \, d\omega. \tag{4.35}$$

The first term of (4.35), $V_{\Lambda\Lambda}(\mid \vec{r}_1 - \vec{r}_2 \mid)$, represents the two-body potential acting between the two Λ-particles. The terms $V_1(r_1)$ and $V_2(r_2)$ represent the interaction between each of the two Λ-particles and the nucleus.

In order to use (4.35), we first need to obtain suitable forms for $V_{\Lambda\Lambda}(\mid \vec{r}_1 - \vec{r}_2 \mid)$, $V_1(r_1)$ and $V_2(r_2)$. Suitable forms for these are discussed in the sections that follow.

We see from (4.35) that the hypercentral potential has the general form

$$\langle U \rangle = \langle V_{12} \rangle + \langle V_{13} \rangle + \langle V_{23} \rangle, \tag{4.36}$$

where $\langle V_{12} \rangle$ represents the two-body potential acting between the two identical Λ-particles. The terms $\langle V_{13} \rangle$ and $\langle V_{23} \rangle$ represent the potential acting between each of the two Λ-particles and the nucleus.

Applying the minimal approximation to (3.44) and (4.17), we end up with a single pair of equations,

$$\begin{cases} \partial_\rho F^{(-)}_{[L_{min}][L'_{min}]}(k,\rho) &= -\dfrac{h^{(+)}_\lambda(k\rho)}{2ik} \langle U \rangle \Big[h^{(-)}_{\lambda''}(k\rho) F^{(-)}_{[L''_{min}][L'_{min}]}(k,\rho), \\ & \quad + h^{(+)}_\lambda F^{(+)}_{[L''_{min}][L'_{min}]}(k,\rho) \Big], \\ \partial_\rho F^{(+)}_{[L_{min}][L'_{min}]}(k,\rho) &= \dfrac{h^{(-)}_\lambda(k\rho)}{2ik} \langle U \rangle \Big[h^{(-)}_{\lambda''}(k\rho) F^{(-)}_{[L''_{min}][L'_{min}]}(k,\rho), \\ & \quad + h^{(+)}_\lambda(k\rho) F^{(+)}_{[L''_{min}][L'_{min}]}(k,\rho) \Big] \end{cases} \tag{4.37}$$

University of South Africa ETD Grobler, J. (2010)

The set of equations (4.37) form the crux of our model.

4.5 $\Lambda\Lambda$-Potential

In our model, we need a two-body potential which describes the interaction between the two Λ-particles. A suitable form for such a potential is (4.38). This potential has been successfully used in few-body calculations [11]. The potential (4.38) represents a weak attraction, having the three-range Gaussian form

$$V_{\Lambda\Lambda}(\rho) = \sum_{i=1}^{3} A_i \exp\,(-\rho^2/\beta_i^2), \tag{4.38}$$

and describes the S-wave interaction of two Λ-particles with the total spin being zero, an S-state. The $\Lambda\Lambda$-potential provides a means of simulating the effect of $\Lambda\Lambda \rightarrow \Xi N$ coupling of the baryon-baryon interaction through modification of the strength of the relevant part of the potential.

The parameters of this potential are listed in Table 4.1.

i	A_i [MeV]	β_i [fm]
1	-21.49	1.342
2	-379.1 $\times\gamma$	0.777
3	9324	0.350

Table 4.1: Parameters of the $\Lambda\Lambda$-potential. The strength of the long-range part of the potential is reduced by multipliying by the factor $\gamma = 0.6598$ in order to ensure agreement with experimental results [11].

The $\Lambda\Lambda$-potential of the type (4.38) is shown in Figure 4.1 for real ρ.

In order to use (4.38), we must ensure that this potential is an analytic function of ρ. This condition enables the potential to be analytically continued

University of South Africa ETD Grobler, J. (2010)

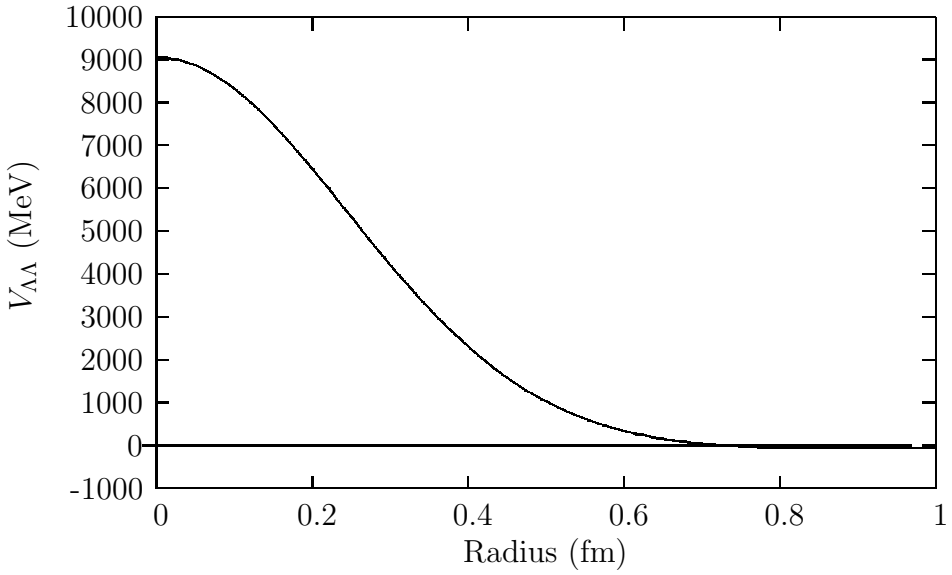

Figure 4.1: ΛΛ-potential. The potential decays exponentially, approaches a negligible value at about 0.7 fm.

from the real axis into the complex ρ-plane. Fortunately, in most cases the model potential has an analytic tail at large distances. In our case the potential is continuous everywhere. For our purposes, it is sufficient to show that (4.38) is an analytic function of ρ by using the following two conditions [28],

$$\lim_{\rho\to 0} \rho^2 V(\rho) = 0,$$

and

$$\lim_{\rho\to 0} \rho V(\rho) = 0.$$

For the first condition we have

$$\begin{aligned}\lim_{\rho\to 0} \rho^2 V_{\Lambda\Lambda}(\rho) &= \lim_{\rho\to 0} \rho^2 \Big[A_1 \exp(-\rho^2/\beta_1^2) + A_2 \exp(-\rho^2/\beta_2^2) + A_3 \exp(-\rho^2/\beta_3^2)\Big] \\ &= 0\end{aligned}$$

and, for the second

University of South Africa ETD Grobler, J. (2010)

$$\lim_{\rho\to\infty} \rho V_{\Lambda\Lambda}(\rho) = \lim_{\rho\to\infty} \rho\Big[A_1 \exp(-\rho^2/\beta_1^2) + A_2 \exp(-\rho^2/\beta_2^2) + A_3 \exp(-\rho^2/\beta_3^2)\Big]$$
$$= 0.$$

Hence, the $\Lambda\Lambda$-potential is less singular at the origin than the centrifugal term, vanishes at infinity faster than the Coulomb potential, and is an analytic function of ρ. Therefore, the potential (4.38) is suitable for our purposes.

4.6 Λ-Nucleus Potential

The Woods-Saxon potential with a well depth of about 30 MeV is seen to describe various orbital angular momentum binding energies for data obtained in emulsion studies [24]. The low momentum transfer reaction,(K^-,π^-), studied with various targets is described reasonably well using the Woods-Saxon potential with a well depth of about 30 MeV. The depth of 30 MeV has been determined from the asymptotic binding energy of the lowest orbital angular momentum for large A. The nuclear medium density is characterized by a Fermi distribution of the form $1 + \exp\Big[(r-c)/a\Big]$.

In (4.35) we use, for $V_1(r_1)$ and $V_2(r_2)$, a Λ-nucleus potential of the Woods-Saxon type (4.39), with a well depth in the region of 30 MeV and which decreases with increasing mass number,

$$V_{\Lambda_1}(r_1) = -\frac{W}{1+\exp\left[(r_1-c)/a\right]}, \tag{4.39}$$

where,

$$c = r_o(A)A^{\frac{1}{3}}. \tag{4.40}$$

It has been shown that a potential of the form (4.35), with a well depth of $W = -28.0$ MeV, radius parameter $r_o = (1.128 + 0.439A^{-\frac{2}{3}})$ fm, and

University of South Africa ETD Grobler, J. (2010)

diffusivity $a = 0.6$ fm, yields a reasonable description of Λ-nucleus single-particle state binding energies [24]. Slightly different values may be used for r_1 and c, but these results are not very sensitive to small variations in these parameters. The Λ-nucleus potential of the type (4.39) is shown in Figure 4.2.

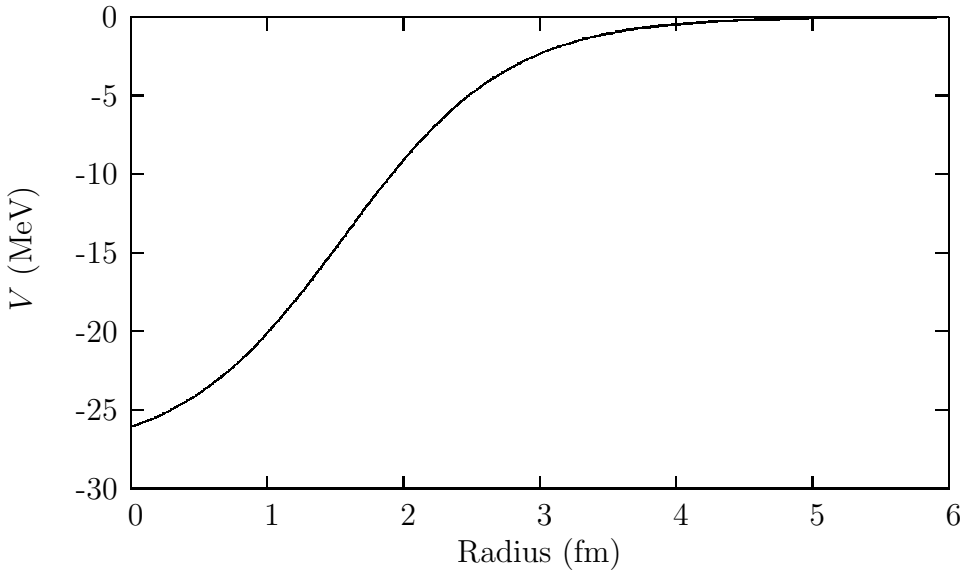

Figure 4.2: Λ-nucleus potential for a well depth of $W = -28.0$ MeV, mass number of $A = 15$ and diffusivity $a = 0.6$ fm. The potential falls off quite rapidly beyond the hypernuclear surface and approaches a negligibly small value at ≈ 5 fm.

University of South Africa ETD Grobler, J. (2010)

The Wood-Saxon potential (4.39) is an analytic function of ρ. Its asymptotic behaviour at short and long distances is

$$\begin{aligned}\lim_{r_1\to 0} r_1^2 V_{\Lambda_1}(r_1) &= \lim_{r_1\to 0}\left[r_1^2 \frac{W}{1+\exp\left[(r_1-c)/a\right]}\right] \\ &= \frac{0}{1+\exp\left[(0-c)/a\right]} \\ &= 0\end{aligned}$$

and,

$$\begin{aligned}\lim_{r_1\to \infty} r_1 V_{\Lambda_1}(r_1) &= \lim_{r_1\to \infty}\left[r_1 \frac{W}{1+\exp\left[(r_1-c)/a\right]}\right] \\ &= 0.\end{aligned}$$

Therefore, the Λ-nucleus potential is less singular at the origin than the centrifugal term, vanishes at infinity faster than the Coulomb potential, and is an analytic function of ρ.

4.7 Total Potential

The total potential for the hypernucleur system is the sum of the Λ-Nucleus potential (4.38) and the $\Lambda\Lambda$-potential (4.39). We therefore combine (4.38) and (4.39) in the hypercentral potential (4.35).

We start with the first term of the intergrand on the right hand side of the integral (4.35). This term can be re-written using (3.33),

$$\begin{aligned}\int V_{\Lambda\Lambda}(\mid \vec{r}_1 - \vec{r}_2 \mid)\, d\omega &= \int V_{\Lambda\Lambda}(\mid \vec{r}_1 - \vec{r}_2 \mid)\left[\frac{1}{4}\sin^2 2\alpha\, d\alpha\right. \\ &\quad \left. \times\, d\Omega_{\vec{r}_1}\, d\Omega_{\vec{r}_1}\right]\end{aligned}$$

University of South Africa ETD Grobler, J. (2010)

$$= \int V_{\Lambda\Lambda}(\mid \vec{r}_1 - \vec{r}_2 \mid)\Bigg[\frac{1}{4}\sin^2 2\alpha\, d\alpha \times(\sin\theta_{\vec{r}_1} d\theta_{\vec{r}_1} d\varphi_{\vec{r}_1})(\sin\theta_{\vec{r}_2}\, d\theta_{\vec{r}_2}\, d\varphi_{\vec{r}_2})\Bigg]. \quad (4.41)$$

The term $\mid \vec{r}_1 - \vec{r}_2 \mid$ in the intergrand of (4.41) represents the physical distance between the two Λ-particles. This term can be re-written as

$$\begin{aligned} \mid \vec{r}_1 - \vec{r}_2 \mid &= \sqrt{r_1^2 + r_2^2 - 2r_1 r_2 \cos\theta} \\ &= \sqrt{\rho^2 - 2\rho^2 \cos\alpha \sin\alpha \cos\theta} \\ &= \rho\sqrt{1 - \sin(2\alpha)\cos\theta}. \end{aligned} \quad (4.42)$$

In order to simplify (4.41), we orient the system with respect to θ_1, with $\theta_1 = \theta$,

$$\theta = \theta_1 \;\Rightarrow\; \int \frac{1}{4}\sin^2(2\alpha)[\sin\theta_{\vec{r}_2}\, d\theta_{\vec{r}_2}\, d\varphi_{\vec{r}_2}]\, d\alpha = 2\pi^2 \int \frac{1}{4}\sin^2 2\alpha,\, d\alpha$$

and hence, (4.41) becomes

$$\begin{aligned} \int V_{\Lambda\Lambda}(\mid \vec{r}_1 - \vec{r}_2 \mid)\, d\omega &= 2\pi^2 \int_0^{\frac{\pi}{2}} d\alpha \int_0^{\pi} \sin\theta\, d\theta\, V_{\Lambda\Lambda}\Big(\rho\sqrt{1 - \sin(2\alpha)\cos\theta}\Big) \\ &\quad \times \sin^2 2\alpha. \end{aligned} \quad (4.43)$$

Using a change of variable, $t = \cos\theta$ in (4.43), with

$$\begin{aligned} dt &= -\sin\theta d\theta, \\ \theta &= 0 \Rightarrow t = 1, \\ \theta &= \pi \Rightarrow t = -1, \end{aligned}$$

and

$$\begin{aligned} \int_0^{\pi} \sin\theta\, d\theta &= -\int_1^{-1} dt \\ &= \int_{-1}^{1} dt, \end{aligned}$$

University of South Africa ETD Grobler, J. (2010)

gives

$$\int V_{\Lambda\Lambda}(\mid \vec{r}_1 - \vec{r}_2 \mid) d\omega = 2\pi^2 \int_0^{\frac{\pi}{2}} d\alpha \int_{-1}^{1} dt\, V_{\Lambda\Lambda}\Big(\rho\sqrt{1-\sin(2\alpha)t}\Big) \times \sin^2 2\alpha. \quad (4.44)$$

Now, considering the integral,

$$\int_{-1}^{1} \exp\Big[-\frac{\rho^2}{\beta^2}(1-\sin 2\alpha)t\Big]\, dt = \exp\Big(-\frac{\rho^2}{\beta^2}\Big) \int_{-1}^{1} \exp\Big(\frac{\rho^2 \sin 2\alpha}{\beta^2} t\Big)\, dt, \quad (4.45)$$

and evaluating the right-hand side of (4.45), we obtain

$$\begin{aligned} \int_{-1}^{1} \exp\Big[-\frac{\rho^2}{\beta^2}(1-\sin 2\alpha)t\Big]\, dt &= \frac{\beta^2}{\rho^2 \sin 2\alpha} \exp\Big(\frac{-\rho^2}{\beta^2}\Big)\Big[\exp\Big(\frac{\rho^2 \sin 2\alpha}{\beta^2} t\Big)\Big]_{-1}^{1} \\ &= \frac{\beta^2}{\rho^2 \sin 2\alpha} \exp\Big(\frac{-\rho^2}{\beta^2}\Big)\Big[\exp\Big(\frac{\rho^2 \sin 2\alpha}{\beta^2}\Big) \\ &\quad - \exp\Big(-\frac{\rho^2 \sin 2\alpha}{\beta^2}\Big)\Big]. \end{aligned} \quad (4.46)$$

Comparing (4.38) with (4.46), we see that each term of (4.38) generates an expression such as (4.46). Therefore, (4.41) may be written in terms of (4.46), as follows

$$\begin{aligned} \int V_{\Lambda\Lambda}(\mid \vec{r}_1 - \vec{r}_2 \mid) d\omega &= \frac{2\pi^2}{\rho^2 \sin^2 2\alpha} \int_0^{\frac{\pi}{2}} \sum_{i=1}^{3} A_i \beta_i \Big\{ \exp\Big[\frac{\rho^2}{\beta_i^2}(1-\sin 2\alpha)\Big] \\ &\quad - \exp\Big[-\frac{\rho^2}{\beta_i^2}(1+\sin 2\alpha)\Big]\Big\} \sin^2 2\alpha\, d\alpha \\ &= 2\pi^2 \int_0^{\frac{\pi}{2}} \sum_{i=1}^{3} A_i \Big(\frac{\beta_i^2}{\rho^2}\Big)\Big\{ \exp\Big[\frac{\rho^2}{\beta_i^2}(1-\sin 2\alpha)\Big] \\ &\quad - \exp\Big[-\frac{\rho^2}{\beta_i^2}(1+\sin 2\alpha)\Big]\Big\} \sin 2\alpha\, d\alpha. \end{aligned} \quad (4.47)$$

Using a change of variable, $X = 2\alpha$ in (4.47), with

$$dX = 2\, d\alpha,$$

University of South Africa ETD Grobler, J. (2010)

$$\alpha = 0 \quad \Rightarrow \quad X = 0,$$

$$\alpha = \frac{\pi}{2} \quad \Rightarrow \quad X = \pi,$$

and

$$\int_0^{\frac{\pi}{2}} 2\alpha \, d\alpha = \int_0^{\pi} dX, \tag{4.48}$$

gives

$$\begin{aligned} \int V_{\Lambda\Lambda}(\mid \vec{r}_1 - \vec{r}_2 \mid) \, d\omega &= \pi^2 \int_0^{\pi} \sum_{i=1}^{3} A_i \Big(\frac{\beta_i^2}{\rho^2}\Big) \Big\{ \exp\Big[-\frac{\rho^2}{\beta_i^2}(1 - \sin X)\Big] \\ &\quad - \exp\Big[-\frac{\rho^2}{\beta_i^2}(1 + \sin X)\Big]\Big\} \sin X \, dX. \end{aligned} \tag{4.49}$$

The second term of the intergral (4.35), which represents the Λ-nucleus potential, may be written using (3.33) as

$$\begin{aligned} \int V_{\Lambda_1}(r_1) \, d\omega &= \int V_{\Lambda_1}(\rho \cos\alpha) \, d\omega \\ &= \int V_{\Lambda_1}(\rho \cos\alpha) \Big[\frac{1}{4} \sin^2 2\alpha \, d\alpha \, d\Omega_{\vec{r}_1} \, d\Omega_{\vec{r}_2}\Big] \\ &= 4\pi^2 \int_0^{\frac{\pi}{2}} V_{\Lambda_1}(\rho \cos\alpha) \sin^2 2\alpha \, d\alpha. \end{aligned} \tag{4.50}$$

Similarily, for the second Λ-particle

$$\int V_{\Lambda_2}(r_1) \, d\omega = 4\pi^2 \int_0^{\frac{\pi}{2}} V_{\Lambda_2}(\rho \sin\alpha) \sin^2 2\alpha \, d\alpha. \tag{4.51}$$

Finally, combining (4.49), (4.50), and (4.51), we obtain the total potential of the hypernuclear system

$$\begin{aligned} \langle U \rangle &= \frac{4m_\Lambda}{\pi\hbar^2} \int_0^{\pi} \Bigg[\Big\{ V_{\Lambda_1}\Big[\rho \cos\Big(\frac{X}{2}\Big)\Big] + V_{\Lambda_2}\Big[\rho \sin\Big(\frac{X}{2}\Big)\Big]\Big\} \sin^2 X \\ &\quad + \sum_{i=1}^{3} A_i \Big(\frac{\beta_i^2}{\rho^2}\Big) \Big\{ \exp\Big[-\frac{\rho^2}{\beta_i^2}(1 - \sin X)\Big] \\ &\quad - \exp\Big[-\frac{\rho^2}{\beta_i^2}(1 + \sin X)\Big]\Big\} \sin X \Bigg] dX, \end{aligned} \tag{4.52}$$

University of South Africa ETD Grobler, J. (2010)

where we have used a change of variable similar to (4.48) in (4.50) and (4.51).

A graphical presentation of the hypercentral potential (4.52) is shown in Figure 4.3.

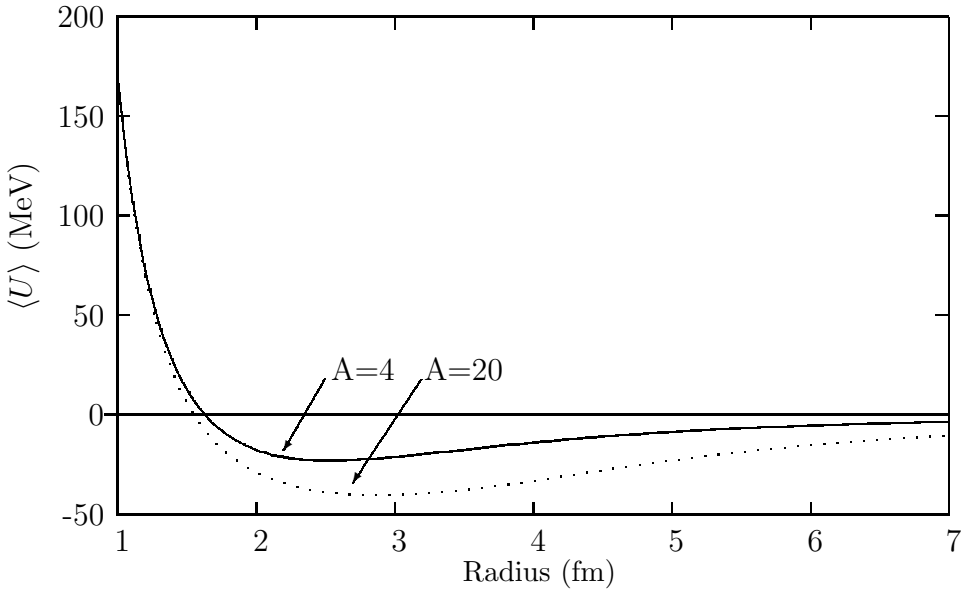

Figure 4.3: Hypercentral potentials for $A = 4 - 20$. The minimum values of the potentials for $A = 4$ and $A = 20$ are about 2.5 fm and 2.8 fm, respectively. Note the increase in depth, $\approx$ 17 MeV, with increasing mass number for $A = 4 - 20$. The minimum of the hypercentral potential for $A = 20$ is shifted by ≈ 0.5 fm relative to that for $A = 4$. The curves for $A = 5 - 19$ lie between the two curves for $A = 4$ and $A = 20$.

The hypercentral potentials (or hyperradial potentials), (4.52), are used as input to the single pair of differential equations, (4.37), in order to determine the two-body Jost functions.

4.8 Complex Rotation

In certain regions of the complex energy plane, limiting values of (4.25) are not achieved when the coupled differential equations (4.37) are integrated

University of South Africa ETD Grobler, J. (2010)

along the real axis. The inherent problem associated with solving the pair of coupled first-order differential equations (4.37) when the potential extends to infinity, is solved by using the complex rotation method [29, 28].

The potentials are analytic functions of the hyperradius, ρ, which is true in many cases and implies that the wave function (4.15) is also an analytic function of ρ. An important property of an analytic function of ρ is that it is independent of the path taken between any two values. In our case, we cannot integrate the differential equations (4.37) along the real axis. The cruical step to solving this problem is to replace the real hyperradius ρ with a complex hyperradius of the form (4.53). This enables integration of (4.37) in the complex plane, along the path from 0 to ρ' as depicted in Figure 4.4.

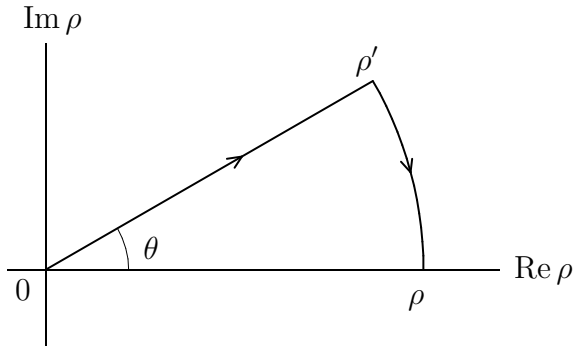

Figure 4.4: Deformed contour showing path of integration for (4.55) with complex energies.

We are concerned only with the asymptotic coefficients, $f^{(-)}_{[L][L']}(k)$ and $f^{(+)}_{[L][L']}(k)$, which are ρ-independent, and are the same for all points on the arc $\rho\rho'$. Therefore, it is sufficient to solve the Schrödinger Equation from the point 0 to ρ'. The arc $\rho\rho'$ desribes rotation of the segment 0 to ρ' on the real axis.

University of South Africa ETD Grobler, J. (2010)

Complex rotation is expressed in terms of the hyperradius as follows

$$\rho = \beta \exp(i\theta), \qquad \beta \geq 0, \tag{4.53}$$

where the interval of the rotation angle θ is

$$0 < |\theta| < \frac{\pi}{2}. \tag{4.54}$$

Using a large enough angle of rotation, θ, we can determine the Jost function at the desired point of interest. The angle should be chosen so that the potential vanishes at the far end of the ray (4.53) sufficiently faster than $1/|\rho'|$. In certain cases, greater $|\rho'|$ values are necessary in order to obtain convergence. Along the ray, at the angle θ, (4.37) is modified, and takes the form

$$\begin{cases} \partial_\beta F^{(-)} &= -\dfrac{e^{i\theta} h_\lambda^{(+)}}{2ik} \langle U \rangle (\beta e^{i\theta}) \Big[h_{\lambda''}^{(-)} F^{(-)} + h_\lambda^{(+)} F^{(+)} \Big], \\ \partial_\beta F^{(+)} &= \dfrac{e^{i\theta} h_\lambda^{(-)}}{2ik} \langle U \rangle (\beta e^{i\theta}) \Big[h_{\lambda''}^{(-)} F^{(-)} + h_\lambda^{(+)} F^{(+)} \Big], \end{cases} \tag{4.55}$$

where the derivatives on the left hand side of (4.55) are taken with respect to the real variable β and additional subscripts and terms have been dropped for the sake of simplicity.

University of South Africa ETD Grobler, J. (2010)

Chapter 5

Results and Discussion

The first-order coupled differential equations (4.55) were solved numerically using the Runge-Kutta method with the total potential (4.52) for the two-Λ hypernuclear system in hyperspherical space. We used the $\Lambda\Lambda$-potential (4.38) and the Λ-nucleus potential (4.39) to construct the total potential of the system.

Binding energies for the ground state, first excited state and the second excited state were obtained for $A = 4 - 20$. The results of our model are given in Table 5.1 and Figure 5.1.

The Λ-Λ binding energy obtained in our results for ${}^{6}_{\Lambda\Lambda}$He is approximately 5.1 MeV, indicating a weak attractive interaction when compared with the Λ-Λ binding energy of $B_{\Lambda\Lambda} = 7.25 \pm 0.19^{+0.18}_{-0.11}$ MeV obtained in the *Nagara* event. The inclusion of the fully-coupled channel baryon-baryon interaction, ΛN-ΣN, would most likely increase the attraction of the system [33].

The Λ-Λ binding energy obtained in our results for ${}^{10}_{\Lambda\Lambda}$Be is approximately 11 MeV, which differs by less than 10% from the experimental value of $B_{\Lambda\Lambda} = 12.33^{+0.35}_{-0.21}$ MeV obtained in the *Demachi-Yanagi* event [12].

University of South Africa ETD Grobler, J. (2010)

A	$B_{\Lambda\Lambda}$ [MeV]	$B^{(1)}_{\Lambda\Lambda}$ [MeV]	$B^{(2)}_{\Lambda\Lambda}$[MeV]
4	-5.094	-0.005	-
5	-6.704	-0.163	-
6	-8.220	-0.421	-
7	-9.641	-0.749	-
8	-10.970	-1.126	-
9	-12.212	-1.542	-
10	-13.376	-2.261	-
11	-14.467	-2.426	-0.045
12	-15.493	-2.889	-0.095
13	-16.457	-3.357	-0.161
14	-17.367	-3.828	-0.241
15	-18.228	-4.298	-0.334
16	-19.042	-4.766	-0.439
17	-19.814	-5.231	-0.555
18	-20.547	-5.691	-0.681
19	-21.244	-6.145	-0.815
20	-21.908	-6.593	-0.956

Table 5.1: Binding energies for the ground states, $B_{\Lambda\Lambda}$, first excited states, $B^{(1)}_{\Lambda\Lambda}$, and the second excited states, $B^{(2)}_{\Lambda\Lambda}$, for $A = 4 - 20$.

University of South Africa ETD Grobler, J. (2010)

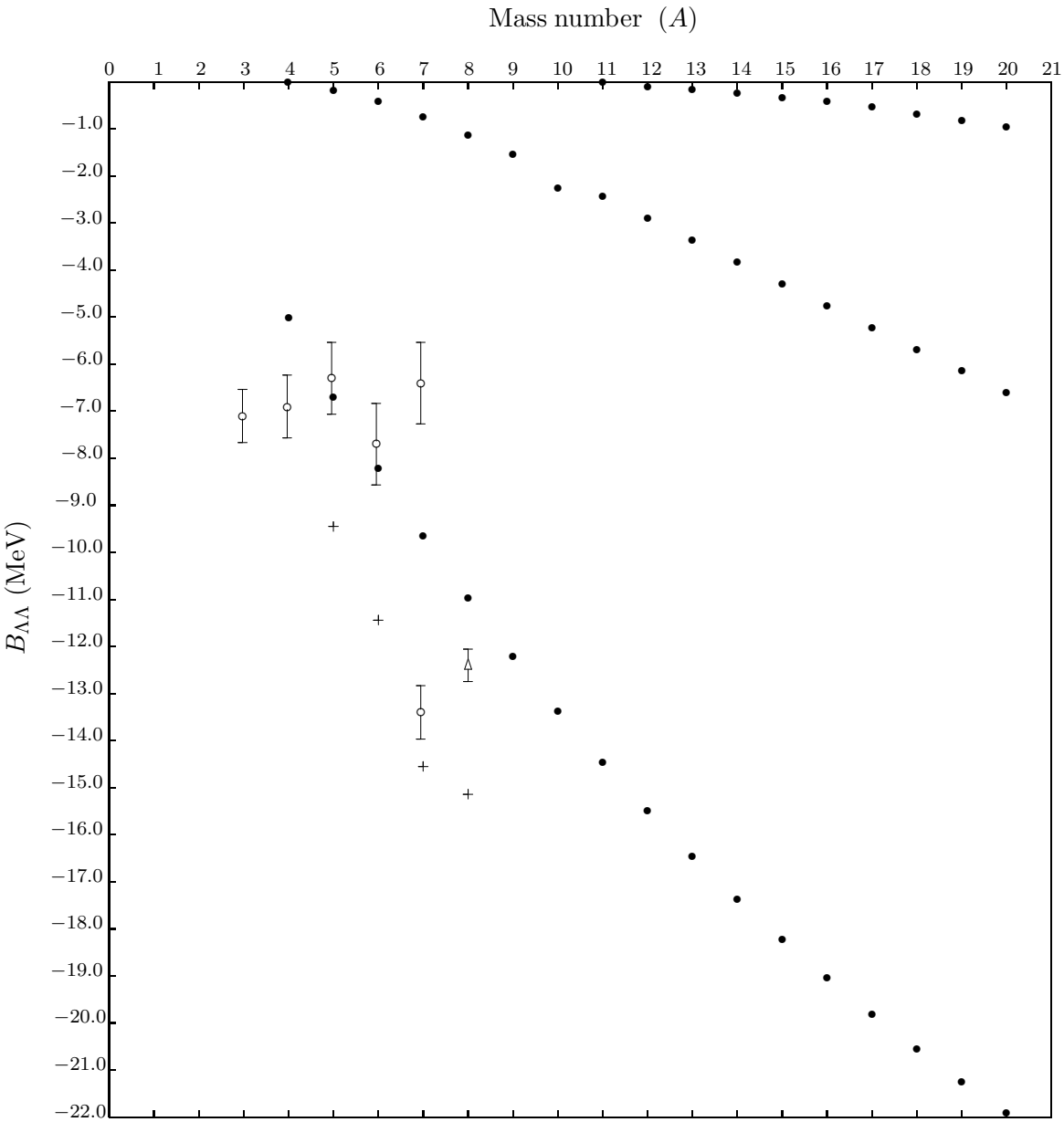

Figure 5.1: Binding energies, $B_{\Lambda\Lambda}$, versus mass number, A, for the ground states, $B_{\Lambda\Lambda}$, first excited states, $B^{(1)}_{\Lambda\Lambda}$, and the second excited states, $B^{(2)}_{\Lambda\Lambda}$, for $A = 4 - 20$. The filled circles are our numerical results, open circles with error bars represent data from the *Nagara* event, the triangle with error bars represents data from the *Demachi-Yanagi* event, and data from the cluster model is indicated using crosses.

University of South Africa ETD Grobler, J. (2010)

The binding energies obtained for ${}^{7}_{\Lambda\Lambda}$He and ${}^{8}_{\Lambda\Lambda}$He are 6.7 MeV and 8.2 MeV, respectively. As can be seen from Figure 5.1, these values are in excellent agreement with the binding energies listed in [7] (See also Table 2.1), thereby indicating the accuracy of our model.

The calculated values in the cluster model [12] show larger values of binding energies for $A = 5 - 8$ when compared with the values obtained in our model. However, our result for $A = 8$ lies closer to the experimental value of $B_{\Lambda\Lambda} = 12.33^{+0.35}_{-0.21}$ MeV obtained in the *Demachi-Yanagi* event, than the value of 15.14 MeV obtained in the Cluster Model (See Table 2.2).

Figure 5.1 shows the variation of binding energy, $B_{\Lambda\Lambda}$, with mass number A. Several features are apparent. First of all, each of the three distinct curves show that the binding energy increases more or less linearly with A. With light hypernuclei, Λ can interact with all of the nucleons in the nucleus, and so $B \propto A$, roughly. As with many other nuclear properties, we may gain valuable clues to the structure of hypernuclei from a systematic study of hypernuclear binding energy. Second, we note that nuclei with large A are more tightly bound, which is not surprising as we know that the magnitude of the nuclear attractive force is directly proportional to the number of nucleons in the nucleus.

In our attempt to understand these curves of binding energy we may use general parameters to characterize the variation of $B_{\Lambda\Lambda}$ with A. The most obvious term to include in estimating $B_{\Lambda\Lambda}$ is a constant term, since $B_{\Lambda\Lambda} \propto A$. The binding energy is then $B_{\Lambda\Lambda} = cA$ where c is a constant to be determined.

We also notice that there are only two bound states for hypernuclei $A = 4-10$ and three bound states for hypernuclei $A = 11 - 20$. The reasons for the apparent increase in the number of bound states for $A > 10$ is due to the

University of South Africa ETD Grobler, J. (2010)

increase in A. An increase in A implies an increasing depth of the attractive potential. The stronger the attractive potential, the more the attraction "pulls-in" the bound states.

We have retained only the first term of the three-body wave function (3.36) in our analysis, the remaining terms were truncated. It can be expected that the inclusion of higher order terms of the three-body wave function may lead to an increase in the binding energy.

University of South Africa ETD Grobler, J. (2010)

Chapter 6

Conclusion

In this work we studied the $\Lambda\Lambda$-hypernuclear system. We described the hypernuclear system using a three-body model within the framework of the hyperspherical coordinate system and solved the system of first order differential equations for the system using the Jost function method.

Comparing our results with the experimental values obtained in the *Nagara* and the *Demachi-Yanagi* events, we estimate the theoretical error in our binding energy calculations of about 1.5 MeV.

Furthermore, we estimate binding energies for $A = 4 - 20$ $\Lambda\Lambda$ hypernuclei, as given in Table 6.1.

Based on the fact that we reproduce the available experimental binding energies reasonably well, we can expect that our results for higher A may serve as predictions for future experiments.

University of South Africa ETD Grobler, J. (2010)

A	$B_{\Lambda\Lambda}$ [MeV]	$B^{(1)}_{\Lambda\Lambda}$ [MeV]	$B^{(2)}_{\Lambda\Lambda}$[MeV]
4	-5.094	-0.005	-
5	-6.704	-0.163	-
6	-8.220	-0.421	-
7	-9.641	-0.749	-
8	-10.970	-1.126	-
9	-12.212	-1.542	-
10	-13.376	-2.261	-
11	-14.467	-2.426	-0.045
12	-15.493	-2.889	-0.095
13	-16.457	-3.357	-0.161
14	-17.367	-3.828	-0.241
15	-18.228	-4.298	-0.334
16	-19.042	-4.766	-0.439
17	-19.814	-5.231	-0.555
18	-20.547	-5.691	-0.681
19	-21.244	-6.145	-0.815
20	-21.908	-6.593	-0.956

Table 6.1: Estimated binding energies for the ground states, $B_{\Lambda\Lambda}$, first excited states, $B^{(1)}_{\Lambda\Lambda}$, and the second excited states, $B^{(2)}_{\Lambda\Lambda}$, for $A = 9 - 20$.

University of South Africa ETD Grobler, J. (2010)

Bibliography

[1] J. H. Rutkowski, *A Brief Story of the Hypernucleus Discovery*, **33**, 11 (2000).

[2] P. E. Hodgson, E. Gadioli, and E. Gadiloi Erba, *Introductory Nuclear Physics* (Oxford University Press, 1997).

[3] M. Danysz, *Hyperfragments*, Nuovo Cimento Suppl. **4**, 609 (1956).

[4] M. Danysz, et. al., Phys. Rev. Lett. **11** 29 (1963); *Nucl. Phys.* **49**, 450 (1964).

[5] D. J. Prowse, Phys. *Rev. Lett.* **17**, 782 (1966).

[6] S. Aoki, et. al., Prog. *Theor. Phys.* **85**, 1287 (1991).

[7] H. Takahashi, et al. *Phys. Rev.* **87**, 212502 (21) (2001).

[8] J. Schaffner-Bielich, *Hypernuclear Physics and compact stars*, astro-ph/0703113.

[9] A. Gal, *Nuclear Physics*, A **804**, 13-24 (2008).

[10] H. Nemura, S. Shinmura, Y. Akaishi, Khin Swe Myint *Phys. Rev.* **94**, 212502 (21) (2005).

[11] I.N. Filikhin, A. Gal, *Nucl. Phys.* A **707**, 491-509 (2002).

University of South Africa ETD Grobler, J. (2010)

[12] E. Hiyama, T. Yamada, *Progress in Particle and Nuclear Physics*, **63**, 339-395 (2009).

[13] E. Hiyama, K. Kamimura, T. Motaba, T. Yamada, Y. Yamamoto, *Phys. Rev.* C **66**, 024007 (2002).

[14] I. N. Filikhin, A. Gal, V. M. Suslov *Nuclear Physics* A **743**, 194-207 (2004).

[15] E. Hiyama, K. Kamimura, T. Motaba, T. Yamada, Y. Yamamoto, *Nuclear Physics* A **738**, 175-181 (2004).

[16] M. Shoeb, A. Mamo, A. Fessahatsion, *Pranama-J. Phys.*, **68**, 6 (2007).

[17] E. Kamimura, *Phys. Rev* A **38**, 621 (1988).

[18] S. N. Nakamura, et. al., *Nuclear Physics* A **754**, 421c-429c (2005).

[19] V. B. Belyaev, S. A. Rakityansky, W. Sandhas, *Nucl. Phys.* A **803**, 210-226 (2008).

[20] C. A. Bertulani, *Nuclear Physics in a Nutshell* (Princeton University Press, 2007).

[21] K. S. Krane, *Introductory Nuclear Physics* (John Wiley & Sons, Inc, 1988).

[22] C. Amsler, et. al.,(Particle Data Group), PL **B667**, 1 (2008) (URL: http://pdg.lbl.gov).

[23] C. Samanta, et. al., Jour. Phys. G: Nucl. Part. Phys. **32**, 363 (2006).

[24] D. J. Millener, C. B. Dover, A. Gal, *Phys. Rev.* C **38**, 2007 (1988).

University of South Africa ETD Grobler, J. (2010)

[25] M. Fabre de la Ripelle, *The potential harmonic expansion method,Ann. Phys.* **147**, 218-320 (1983).

[26] A. F. Taylor, *Scattering Theory*, (John Wiley & Sons, Inc., New York, 1972).

[27] M. Abramowitz, A. Stegun, *Handbook of Mathematical Functions* (NBS, Washington, 1964).

[28] S. A. Rakityansky, S. A. Sofianos, K. Amos *Nuovo Cim.* B **111**, 363-378 (1996).

[29] S. A. Sofianos, S. A. Rakityansky, G. P. Vermaak *Nucl. part. Phys.* **23**, 1619-1629 (1997).

[30] D. G. Zill and M. R. Cullen, *Differential Equations with Boundary-Value Problems*, 4th ed. (International Thompson Publishing, 1997).

[31] S. A. Rakityansky, S. A. Sofianos *J. Phys.* A: *Math. Gen.* **31**, 5149-5175 (1998).

[32] E. Merzbacher, *Quantum Mechanics*, 3rd ed., (John Wiley & Sons, Inc., 1998).

[33] E. Hiyama, *Weakly bound states in hypernuclei*, Few-Body Syst. **34**, 79-84 (2004).